Brain-wide cellular resolution imaging of Cre transgenic zebrafish lines for functional circuit-mapping

Kathryn M. Tabor[1], Gregory D. Marquart[1,2], Christopher Hurt[1,3], Trevor S. Smith[1], Alexandra K. Geoca[1], Ashwin A. Bhandiwad[1], Abhignya Subedi[1,4], Jennifer L. Sinclair[1], Nicholas F. Polys[3], and Harold A. Burgess[1*]

[1] Division of Developmental Biology, *Eunice Kennedy Shriver* National Institute of Child Health and Human Development, Bethesda, MD, USA

[2] Neuroscience and Cognitive Science Program, University of Maryland, College Park, MD 20742.

[3] Advanced Research Computing, Department of Computer Science, Virginia Polytechnic Institute and State University, 3050 Torgersen Hall, Blacksburg, VA, USA

[4] Postdoctoral Research Associate Training Program, National Institute of General Medical Sciences, Bethesda, MD, USA

* Correspondence: burgessha@mail.nih.gov ; 301-402-6018

Keywords: Cre, Gal4, intersectional genetics, brain atlas, zebrafish

Abstract

Decoding the functional connectivity of the nervous system is facilitated by transgenic methods that express a genetically encoded reporter or effector in specific neurons; however, most transgenic lines show broad spatiotemporal and cell-type expression. Increased specificity can be achieved using intersectional genetic methods which restrict reporter expression to cells that co-express multiple drivers, such as Gal4 and Cre. To facilitate intersectional targeting in zebrafish, we have generated more than 50 new Cre lines, and co-registered brain expression images with the Zebrafish Brain Browser, a cellular resolution atlas of 264 transgenic lines. Lines labeling neurons of interest can be identified using a web-browser to perform a 3D spatial search (zbbrowser.com). This resource facilitates the design of intersectional genetic experiments and will advance a wide range of precision circuit-mapping studies.

Introduction

Elucidating the functional circuitry of the brain requires methods to visualize neuronal cell types and to reproducibly control and record activity from identified neurons. Genetically encoded reporters and effectors enable non-invasive manipulations in neurons but are limited by the precision with which they can be targeted. While gene regulatory elements are often exploited to direct transgene expression, very few transgenic lines strongly express reporter genes in a single cell type within a spatially restricted domain. Precise targeting of optogenetic reagents can be achieved using spatially restricted illumination in immobilized or optic-fiber implanted animals (Aravanis et al., 2007; Arrenberg et al., 2009; Zhu et al., 2012). However, non-invasive genetic methods that confine expression to small groups of neurons enable analysis of behavior in freely moving animals. Such methods include intersectional genetic strategies, where reporter expression is controlled by multiple independently-expressed activators (Dymecki et al., 2010; Gohl et al., 2011).

In zebrafish, intersectional control of transgene expression has been achieved by combining the Gal4/UAS and Cre/lox systems (Forster et al., 2017; Satou et al., 2013; Tabor et al., 2018). Gal4-Cre intersectional systems take advantage of hundreds of existing Gal4 lines which are already widely used in zebrafish circuit neuroscience (Asakawa et al., 2008; Bergeron et al., 2012; Scott et al., 2007), but are limited by the relatively poor repertoire of existing Cre lines, and difficulty in identifying pairs of driver lines that co-express in neurons of interest. The first version of the Zebrafish Brain Browser (ZBB) atlas provided a partial solution to these problems by co-aligning high resolution image stacks of more than 100 transgenic lines, with an accuracy approaching the limit of biological variability (Marquart et al., 2017, 2015). ZBB enabled users to conduct a 3D spatial search for lines with reporter expression in areas of interest and predict the area of intersect between Gal4 and Cre lines, aiding the

design of intersectional genetic experiments. However, ZBB software required local installation and only included 9 Cre lines, limiting opportunities for intersectional targeting.

Here, we describe the ZBB2 atlas, which comprises whole-brain expression patterns for 264 transgenic lines, including 65 Cre lines, and 158 Gal4 lines. We generated more than 100 new enhancer trap lines that express Cre or Gal4 in diverse subsets of neurons, then registered a high resolution image of each to the original ZBB atlas. For 3D visualization of expression patterns and to facilitate spatial searches for experimentally useful lines, we now provide an online interface to the atlas. Collectively, ZBB2 labels almost all cellular regions within the brain and will facilitate the reproducible targeting of neuronal subsets for circuit-mapping studies.

Results

To accelerate discovery of functional circuits we generated a library of transgenic lines that express Cre in restricted patterns within the brain and built an online 3D atlas (Fig. 1). New Cre lines were generated through an enhancer trap screen: we injected embryos with a Cre vector containing a basal promoter that includes a neuronal-restrictive silencing element to suppress expression outside the nervous system, and tol2 transposon arms for high efficiency transgenesis (*REx2-SCP1:BGi-Cre-2a-Cer*) (Bergeron et al., 2012; Kawakami, 2007; Marquart et al., 2015). In injected G0 embryos, the reporter randomly integrates into the genome such that Cre expression is directed by local enhancer elements. To isolate lines with robust brain expression in relatively restricted domains, we visually screened progeny of G0 adults crossed to the *βactin:Switch* transgenic line that expresses red fluorescent protein (RFP) in cells with Cre (Horstick et al., 2014). We retained 52 new lines that express Cre in restricted brain regions at 6 days post-fertilization (dpf), the stage most frequently used

for behavioral experiments and circuit-mapping. We then used a confocal microscope to scan brain-wide GFP and RFP fluorescence from *et-Cre, βactin:Switch* larvae at high resolution, aligned the merged signal to the ZBB *βactin:GFP* pattern and applied the resulting transformation matrix to the RFP signal alone. To obtain a representative image of Cre expression, we averaged registered brain scans from 3-10 larvae and masked expression outside the brain. Cre lines reported here for the first time are shown in Fig. 2, and an overview of all 65 Cre lines that can be searched using ZBB2 is summarized in Table S1.

We previously isolated more than 200 Gal4 lines with expression in subregions of the brain; however, the original ZBB atlas represented only those that showed expression restricted to the nervous system. The subsequent development of a synthetic untranslated region (UTR.zb3) that suppresses non-neuronal expression has mitigated issues associated with Gal4 driving effector genes in non-neuronal tissues (Marquart et al., 2015). We therefore imaged 45 additional Gal4 lines in which robust brain expression is accompanied by expression in non-neural tissues. We visualized Gal4 expression using the *UAS:Kaede* transgenic line and registered patterns to ZBB by co-imaging *vglut2a:DsRed* expression. New Gal4 lines reported here are shown in Fig. 3. We also aligned 20 high resolution brain scans of Gal4 lines performed by either the Dorsky or Baier laboratories by adapting a method for multi-channel registration of the Z-Brain and ZBB atlases (Forster et al., 2017; Marquart et al., 2017; Otsuna et al., 2015). In total, ZBB2 includes the spatial pattern of expression for 158 Gal4 lines. Table S2 summarizes all Gal4 enhancer traps generated by our laboratory that can be searched in ZBB2. In total, ZBB2 describes the expression pattern for 264 transgenic lines, more than doubling the number in the original atlas (Table 1).

Enhancer traps randomly integrate into the genome and it is not usually possible to determine the identity of the cells labeled by their spatial pattern of expression alone. However, cell-type information for enhancer trap lines can be inferred from co-localization with reporters whose expression is directed by a defined promoter, or through integration into a bacterial artificial chromosome. ZBB2 contains expression data for 56 such transgenic lines, including reporters for most major neurotransmitters. Additional cell type information in enhancer trap lines may be revealed by integration site mapping, because enhancer traps often recapitulate the expression pattern of genes close to the site of transgene integration. We therefore developed a new method to efficiently map integration sites, using an oligonucleotide to hybridize with the enhancer trap tol2 arms and capture flanking genomic DNA fragments for sequencing (see Methods for detail). We recovered the integration site for 55 Gal4 and Cre enhancer trap lines (detailed in Tables S1 and S2). Altogether 171 of the lines in ZBB2 either use a defined promoter, or have a known genomic integration site, providing molecular genetic information on cell-type identity.

To assess how useful the lines represented in ZBB2 will be for circuit-mapping studies, we calculated the selectivity of each line. For this, we first estimated the volume of the brain that includes cell bodies — using transgenic markers of cell bodies and neuropil (Fig. 4A) — then calculated the percent of the cell body volume labeled by each line. For Cre lines, median coverage of the cell body volume was 6% (range 0.1 to 48%, Fig. 4B,D). As we estimate that there are ~92,000 neurons in the 6 dpf brain (see Methods), this equates to a median of around 5500 neurons per line. In total, 96% of the cellular volume is labeled by at least one Cre line, with an average of 6 lines per voxel. However, Cre lines provide limited access to the midbrain tegmentum, posterior tuberculum and trigeminal ganglion (Fig. 4B). Gal4 lines tend to have more restricted expression than Cre lines, with a median coverage of 1% (range 0.02 to 29%, ~900 neurons per line). Collectively Gal4 lines label 91% of the cell body volume

(Fig. 4C,D). Salient areas that are not labeled include a rostro-dorsal domain of the optic tectum, the caudal lobe of the cerebellum, and a medial area within rhombomeres 3-4 of the medulla oblongata. Despite Gal4 lines having more restricted expression, few show tightly confined expression, highlighting the importance of intersectional approaches for precise targeting.

For the first release of the ZBB atlas, we provided downloadable *Brain Browser* software that allowed users to conduct a 3D spatial search for transgenic lines that label neurons within a specific Z-Brain defined neuroanatomic region (Randlett et al., 2015) or selected volume. For ZBB2, we have imported all the new lines into the original *Brain Browser*. However, recognizing that requiring a locally installed IDL runtime platform posed a limit to accessibility, we implemented an online version that can be accessed using a web-browser (http://zbbrowser.com). The online version includes key features of the original *Brain Browser*, including 3D spatial search, prediction of the area of intersectional expression between selected lines, partial/maximal/3D projections, information about the neuroanatomical identity of any selected voxel and ability to load user-generated image data (Fig. 5). Additionally, the online version features an integrated virtual reality viewer for Google cardboard. We used X3DOM libraries to achieve rapid volume rendering and enable users to select data resolution that best matches their connection speed, so that the browser-based implementation remains highly responsive (Arbelaiz et al., 2017b, 2017a). Both local and web-based versions include hyper-links to PubMed, UCSC Genome Browser and Zfin, so that users can quickly retrieve publications describing each line, its integration site, and ordering information, respectively.

Discussion

The ZBB2 atlas provides cellular resolution imaging data for 65 Cre lines, and 158 Gal4 lines, enabling small clusters of neurons to be genetically addressed through intersectional targeting. To aid in the design of such experiments, we have implemented a web-based interface that allows users to perform a spatial search for lines that express Cre or Gal4 in any selected 3D volume, and thereby identify transgenic lines for intersectional visualization or manipulation of selected neurons (Tabor et al., 2018). We anticipate that the ZBB2 lines will also facilitate structural mapping of the zebrafish brain because many strongly label discrete neuroanatomical entities.

In *Drosophila*, intersectional genetic targeting is often achieved using 'split' systems (Gal4, lexA and Q) in which the DNA-binding domain and transactivation domain of a transcription factor are separately expressed ensuring that activity is reconstituted only in neurons that express both protein domains during the same time interval (Pfeiffer et al., 2010; Ting et al., 2011; Wei et al., 2012). We did not pursue this approach because of the investment needed to create and maintain numerous 'half' lines which can not be used alone. In contrast, Gal4 and Cre lines are independently useful and Cre lines can be used intersectionally with hundreds of existing zebrafish Gal4 lines. Several intersectional reporter lines have already been generated to visualize cells that co-express Cre and Gal4 (Forster et al., 2017; Satou et al., 2013). In addition, the *UAS:KillSwitch* line enables selective ablation of neurons that co-express Gal4 and Cre, and the *UAS:DoubleSwitch* line sparsely labels neurons within a Gal4/Cre co-expression domain for morphological reconstruction (Tabor et al., 2018).

A limitation of the Cre system is that insufficient expression may lead to stochastic activity at target loxP sites and consequent mosaic reporter expression (Forster et al., 2017; Schmidt-Supprian and Rajewsky, 2007). We therefore only retained lines with strong expression across multiple animals. Conversely Cre is toxic at high levels — in some cases, mosaic expression may be due to the death of a

subset of cells (Bersell et al., 2013). While we cannot readily assess the toxicity of our lines, confounding effects can be experimentally addressed with the proper controls. Our enhancer trap Cre lines tend to have broader expression than Gal4 lines, likely because (1) Cre expression in progenitor cells labels all offspring, expanding the domain of expression, and (2) switch reporters remain active after transient Cre expression, whereas Gal4 must be continually expressed to drive UAS reporters. Occasionally we have observed UAS:Switch expression in neurons outside the domain of Cre expression in the ZBB2 atlas. This may be because the 14xUAS-E1b promoter is stronger than the β-actin promoter present in the switch reporter used to build the atlas. Additionally, most brain regions contain multiple cell types with biological variability in their precise position. Thus predicted overlapping expression based on co-registered brain scans must be experimentally verified.

The ZBB2 atlas advances mapping of the zebrafish brain at single cell resolution by comprehensively describing the cellular-resolution pattern of brain expression for 264 transgenic lines and providing a user-friendly web-browser based interface for searching and visualizing the expression in each. New Cre and Gal4 enhancer trap lines are freely available and we anticipate will advance circuit-mapping studies by providing essential reagents for intersectional targeting of neurons. We expect that this database and the associated transgenic lines will drive exploration of structure/function relations in the vertebrate brain.

Methods

Husbandry

Zebrafish (*Danio rerio*) were maintained on a Tubingen long fin strain background. Larval zebrafish were raised on 14/10 h light/dark cycle at 28 °C in E3h medium (5 mM NaCl, 0.17 mM KCl, 0.33 mM

179 CaCl2, 0.33 mM MgSO4, 1.5 mM HEPES, pH 7.3) with 300 μM N-Phenylthiourea (PTU, Sigma) to
180 suppress melanogenesis for imaging. Experiments were conducted with larvae in the first 7 days post
181 fertilization (dpf), before sex differentiation. Experimental procedures were approved by the NICHD
182 animal care and use committee.
183
184 Zebrafish lines
185 Enhancer trap lines that express Cre (*et-Cre* lines) were initially isolated through enhancer trap
186 screening using a tol2 vector containing a REx2-SCP1:BGi-Cre-2a-Cer cassette (286 adult fish
187 screened) (Marquart et al., 2015). Although the fluorescent protein Cerulean is co-expressed with Cre
188 in this vector, it was rarely strong enough to visualize directly, and we instead screened using the
189 *βactin:Switch* transgenic line (Horstick et al., 2014). Thus subsequently, we removed the 2a-Cer
190 cassette from the enhancer trap vector for generating new lines and injected a vector with a REx2-
191 SCP1:BGi-Cre cassette (75 adult fish screened). At least 50 (usually over 100) offspring of injected fish
192 were visually screened for RFP fluorescence from the *βactin:Switch (Tg(actb2:loxP-eGFP-loxP-ly-*
193 *TagRFPT)y272)* reporter line (Horstick et al., 2014). As around 10% of injected animals transmitted
194 more than a single expression pattern, likely reflecting several integration loci, we bred each line for
195 multiple generations to isolate a single heritable transgene. Because we only retained lines with
196 restricted areas of brain expression, we ultimately kept lines from around 20% of injected fish. For
197 maintenance, Cre lines were crossed to fish heterozygous for the *βactin:Switch* transgene. Outcrossing
198 to *βactin:Switch* was necessary because, as in other systems, leaky Cre expression recombines lox sites
199 that are transmitted through the same gamete (Schmidt-Supprian and Rajewsky, 2007). Consequently,
200 in clutches from *et-Cre;βactin:Switch* crossed to *βactin:Switch*, we discarded ~25% of embryos that
201 showed ubiquitous RFP expression due to complete recombination of the Switch reporter in gametes
202 also containing the Cre transgene. We also imaged previously described Cre lines with rhombomere-

specific expression (Tabor et al., 2018). Gal4 enhancer trap lines were isolated as previously described (Bergeron et al., 2012).

Other zebrafish lines in this study were: *UAS:Kaede (Tg(UAS-E1b:Kaede)s1999t* (Davison et al., 2007)*, y379-Cre* and *y484-Cre* (Marquart et al., 2017)*, vglut2a:DsRed (TgBAC(slc17a6b:loxP-DsRed-loxP-GFP)nns9) (Satou et al., 2013)*, *Tg(gata1:dsRed)sd2* (Traver et al., 2003), *Tg(-4.9sox10:EGFP)ba2* (Wada et al., 2005), *Tg(-8.4neurog1:GFP)sb1* (Blader et al., 2003), *Tg(kctd15a:GFP)y534* (Heffer et al., 2017), *Tg(pou4f3:gap43-GFP)s356t* (Xiao et al., 2005)*, Et(-1.5hsp70l:Gal4-VP16)s1156t* and *Et(fos:Gal4-VP16)s1181t* (Scott and Baier, 2009), *TgBAC(neurod:EGFP)nl1* (Obholzer et al., 2008)*, Tg(mnx1:GFP)ml2* (Flanagan-Steet et al., 2005), and *y271-Gal4 (Horstick et al., 2014)*. For counting neurons in the brain, we used *huC:h2b-GCaMP6* (*Tg(elavl3:h2b-GCaMP6)jf5*) (Vladimirov et al., 2014), which has multiple transgene integrations, minimizing effects of variable expression and silencing.

Brain imaging and processing

For imaging, 6 dpf larvae were embedded in 1.5 – 3.5 % agarose in E3h and oriented dorsal to the objective. Each larval brain was scanned in 2 image stacks (anterior and posterior halves, 1x1x2 µm resolution) with an inverted Leica TCS-SP5 II confocal with a 25X, 0.95 NA objective, while adjusting laser power during scans to compensate for intensity loss with depth. Gal4 expression was visualized using *UAS:Kaede* and Cre expression using RFP expression from *βactin:Switch.* Color channels were usually acquired simultaneously and crosstalk removed in post-processing using a Leica dye separation algorithm. Substacks were connected using the pairwise stitching plugin in ImageJ (Preibisch et al., 2009; Schneider et al., 2012).

Image registration was performed using affine and diffeomorphic algorithms in ANTs (Avants et al., 2011) with parameters optimized for live embryonic zebrafish brain scans that produce alignments with an accuracy of approximately one cell diameter (8 µm) (Marquart et al., 2017). For registration, each image stack required a reference image previously registered to the ZBB coordinate system. Reference channels were *vglut2a:DsRed* for Gal4 lines and *βactin:Switch* GFP for Cre lines. Other transgenic lines and patterns were registered using either *vglut2a:dsRed* or *vglut2a:GFP* where appropriate. For Cre lines, we merged the *βactin:Switch* GFP and RFP signals into a combined pattern to provide a channel for registration. We then applied the resulting transformation matrix to the RFP channel alone. Next, we averaged registered brain images from at least 3 larvae per line, using the ANTs *AverageImages* command, to create a representative image of each line. Mean images were masked to remove expression outside the brain, except where inner ear hair cells or neuromasts were labeled. Next, we normalized intensity to saturate the top 0.01% of pixels, and downsampled to 8-bit to reduce file size and facilitate distribution. We manually defined fluorescent intensity thresholds for each line that best distinguished cellular expression from neuropil or background to facilitate spatial search for lines that express in selected cell populations. Mean images were also aligned to Z-Brain using a previously described bridging transformation matrix (Marquart et al., 2017).

Because registration using the *βactin:Switch* bridging channel proved more accurate than our previous bridging registration with *HuC:Cer*, we re-imaged and registered the Cre lines recovered in our pilot screen. Gal4 lines generated and imaged by the Dorsky lab (Otsuna et al., 2015) were registered using two channels: the nuclear counter-stain channel (TO-PRO®-3) and immunolabeling for myosin heavy chain, aligned to *HuC:nls-mCar* and *tERK* in ZBB respectively. We also used multichannel registration to align brain scans performed by the Baier lab (Forster et al., 2017), taking advantage of three expression patterns present in both datasets: v*glut2a:dsRed*, *isl2b:GFP* and *gad1b:GFP*.

251

252 Integration site mapping

253 To efficiently map enhancer trap integration sites we extracted genomic DNA from embryos from each
254 line (Qiagen DNeasy Blood and Tissue Kit) and generated a barcoded library. We hybridized the library
255 to biotinylated 120 bp primers (IDT ultramers) designed against the tol2 sequence arms and enriched
256 for genomic integration sites using avidin-pulldown. Enriched libraries were combined into 15 pools
257 such that each pool contained a unique combination of five transgenic lines and each line was
258 exclusively represented in two pools. Pooled libraries were sequenced using an Illumina MiSeq
259 (Illumina) which produced 250 bp paired-end reads. Reads were aligned against the biotinylated primer
260 sequence, then unique sequences within each read subsequently aligned to a zebrafish reference
261 genome (danRer10). Sequences common to all pools were assumed to be off-target and removed from
262 analysis. Remaining reads from each pool were cross-referenced to the combination of embryos in each
263 pool. Regions that had high and specific enrichment in both pools containing DNA from a particular
264 sample were assigned as candidate insertion sites for that sample. To validate this procedure, we
265 confirmed the map position for 4 lines through direct PCR genotyping.

266

267 Expression analysis

268 To assess the selectivity of transgene expression, we manually set an intensity threshold for each line to
269 distinguish cell body labeling from background, and calculated the proportion of voxels in the total cell
270 body volume with a super-threshold signal. In assessing total brain coverage by the Cre library, we
271 excluded *y457-Cre* which has extremely broad (possibly pan-neuronal) expression.

272

To estimate the total number of cells at 6 dpf, we dissected brains and counted dissociated cells using a cell sorter, yielding a total of 124700 ± 2200 cells per brain (mean and standard error, N = 9), including mature and immature neurons, glia and non-neural cells (e.g. connective tissue and vasculature). For this procedure, brains were dissected at room temperature in 1x PBS (K-D Medical), dissociated in papain (Papain Dissociation System, Worthington Biochemical) by incubation in 20 U/mL papain for 20 min then triturated and 0.005% DNAse added. The final volume was adjusted to 200 µL in DMEM fluorobrite (Gibco) and immediately counted using a BD FACSCalibur (BD Biosciences), using a custom gate to include single cells in the forward and side scattered area. To minimize cell death, the entire process was completed within 45 min per brain.

We estimated the number of differentiated neurons by manually counting fluorescently labeled post-mitotic neurons in brain images. For this, we first imaged *huC:h2b-GCaMP6* transgenic brains at high-resolution (0.5 × 0.5 × 0.5 µm per voxel). In this line, nuclear-localized GCaMP fluorescence provides a discrete signal that facilitates identification of single neurons even in dense regions. We assigned all voxels in the brain to 5 neuronal-density bins based on the ratio of *huC:nls-mCar* (somas), and *huC:Gal4, UAS:syp-RFP* (synapses ; see Fig. 4A) and identified five representative volumes (30 × 30 × 30 µm each) for each of the five bins. We then counted neurons in *huC:h2b-GCaMP6* brain scans in each of the 25 volumes. Finally, we scaled the mean number of neurons in each bin by the relative fraction of the brain that each bin covers to obtain an estimate of the total neuron number. Using this procedure, we estimated that there are 92,000 ± 3000 mature neurons in the 6 dpf brain (N = 3 larvae).

Zebrafish Brain Browser Software

The lines scanned and registered here were incorporated into the locally run Zebrafish Brain Browser, which requires downloading an installing the free IDL runtime environment. ZBB2 (including software

297 and full resolution datasets) can be downloaded from our website
298 (http://helix.nih.gov/~BurgessLab/zbb2.zip).
299
300 To increase accessibility we also implemented an online version of ZBB2 that does not require
301 downloading, and runs in any javascript-enabled web-browser (http://zbbrowser.com). We used
302 Bootstrap (http://getbootstrap.com/) for interface design and jQuery for event-handling
303 (https://jquery.com/). For rendering of 2D slices and 3D projections, we used X3DOM, a powerful set
304 of open-source 3D graphics libraries for web development which integrates the X3D file format into
305 the HTML5 DOM (Behr et al., 2009; Congote, 2012; John et al., 2007; Polys and Wood, 2012). ZBB2
306 uses X3DOM's built in *MPRVolumeStyle* and *BoundaryEnhancementVolumeStyle* functions to render
307 2D image files (texture atlases) in 3D space. The *MPRVolumeStyle* is used for the X, Y and Z slicer
308 views to display a single slice from a 3D volume along a defined axis. We modified X3DOM source
309 code for this volume style to support additional features including color selection, contrast and
310 brightness controls, rendering of crosshairs, spatial search boxes and intersections between selected
311 lines. The *BoundaryEnhancementVolumeStyle* renders the 3D projection. We also modified this
312 function's source code, including additions of color, contrast, and brightness values. Other minor
313 changes were made to the X3DOM libraries including a hardcoded override to allow additive blending
314 of line colors. The online ZBB2 loads images of each line as a single 2D texture atlas. Image volumes
315 for each line were converted to a montage, downsampling by taking every 4th plane in the z-dimension,
316 and to 0.25, 0.5, and 0.75 their original size for low, medium, and high resolutions respectively to
317 ensure rapid loading time. Texture atlas images were then referenced using X3DOM's
318 "ImageTextureAtlas" node, and its "numberOfSlices", "slicesOverX", and "slicesOverY" attributes
319 were specified as 100, 10, and 10, respectively. These atlases were then referenced by "VolumeData"

nodes, along with an *MPRVolumeStyle* or *BoundaryEnhancementVolumeStyle* node, to build the volumes visible on the screen.

To implement the 3D spatial search in the online edition of ZBB2, we first binarized and 4x-downsampled the resolution of each line. The data for each line was then parsed into a single array (width, height, depth). We compressed adjacent binary values into a single byte using bit shifting operators, downsampling the data once again by 8 times. While greatly downsized, the entire dataset was still much too large to quickly download. We therefore fragmented the array for each line into 8x8x8 blocks of 64 bytes each, and concatenated blocks for every line, creating a single array of around 17 kb for a specific sub-volume of the brain. After the user defines the search volume, relevant volume fragments are downloaded and searched. Data from each fragment file is passed to a JavaScript Web Worker, allowing each file to be searched in a separate thread. This procedure facilitates minimal search times, with the main limitation being that thousands of binary files must be regenerated whenever a new line is added to the library.

Quantification and Statistical Analysis

Analysis was performed with IDL (http://www.harrisgeospatial.com/SoftwareTechnology/IDL.aspx), Gnumeric (http://projects.gnome.org/gnumeric/) and Matlab (Mathworks).

Resource sharing

Most enhancer trap lines are available from Zebrafish International Resource Center (https://zebrafish.org), with all others available from the authors upon request. Registered individual confocal brain scans can be downloaded from Dryad (http://datadryad.org/review?

343 doi=doi:10.5061/dryad.tk467n8). Brain browser javascript code can be downloaded from GitHub
344 (https://github.com/BurgessLab/ZebrafishBrainBrowser)
345
346 **Acknowledgments**
347
348 We thank Steven Coon and James Iben from the NICHD Molecular Genomics Core and Lisa Williams-
349 Simons from the NICHD FACS core for vital assistance. We are grateful to Jeremy Swan for help with
350 interface design. This study utilized the high-performance computational capabilities of the Biowulf
351 Linux cluster at the National Institutes of Health, Bethesda, MD (http://biowulf.nih.gov). The authors
352 acknowledge Advanced Research Computing at Virginia Tech for providing computational resources
353 and technical support that have contributed to the results reported within this paper
354 (http://www.arc.vt.edu). This work was supported by the Intramural Research Program of the *Eunice*
355 *Kennedy Shriver* National Institute for Child Health and Human Development.
356
357 **Competing interests**
358
359 The authors declare no conflict of interest.
360
361 **References**
362

Aravanis AM, Wang L-P, Zhang F, Meltzer LA, Mogri MZ, Schneider MB, Deisseroth K. 2007. An optical neural interface: in vivo control of rodent motor cortex with integrated fiberoptic and optogenetic technology. *J Neural Eng* **4**:S143-156. doi:10.1088/1741-2560/4/3/S02

Arbelaiz A, Moreno A, Kabongo L, García-Alonso A. 2017a. X3DOM volume rendering component for web content developers. *Multimed Tools Appl* **76**:13425–13454. doi:10.1007/s11042-016-3743-1

Arbelaiz A, Moreno A, Kabongo L, Polys N, García-Alonso A. 2017b. Community-driven Extensions to the X3D Volume Rendering ComponentProceedings of the 22Nd International Conference on 3D Web Technology, Web3D '17. New York, NY, USA: ACM. pp. 1:1–1:9. doi:10.1145/3055624.3075945

Arrenberg AB, Del Bene F, Baier H. 2009. Optical control of zebrafish behavior with halorhodopsin. *Proc Natl Acad Sci U A* **106**:17968–73. doi:10.1073/pnas.0906252106

Asakawa K, Suster ML, Mizusawa K, Nagayoshi S, Kotani T, Urasaki A, Kishimoto Y, Hibi M, Kawakami K. 2008. Genetic dissection of neural circuits by Tol2 transposon-mediated Gal4 gene and enhancer trapping in zebrafish. *Proc Natl Acad Sci USA* **105**:1255–1260. doi:10.1073/pnas.0704963105

Avants BB, Tustison NJ, Song G, Cook PA, Klein A, Gee JC. 2011. A reproducible evaluation of ANTs similarity metric performance in brain image registration. *NeuroImage* **54**:2033–2044. doi:10.1016/j.neuroimage.2010.09.025

Behr J, Eschler P, Jung Y, Zöllner M. 2009. X3DOM: A DOM-based HTML5/X3D Integration ModelProceedings of the 14th International Conference on 3D Web Technology, Web3D '09. New York, NY, USA: ACM. pp. 127–135. doi:10.1145/1559764.1559784

Bergeron SA, Hannan MC, Codore H, Fero K, Li G, Moak ZB, Yokogawa T, Burgess HA. 2012. Brain selective transgene expression in zebrafish using an NRSE derived motif. *Front Neural Circuits* **6**:110. doi:10.3389/fncir.2012.00110

Bersell K, Choudhury S, Mollova M, Polizzotti BD, Ganapathy B, Walsh S, Wadugu B, Arab S, Kuhn B. 2013. Moderate and high amounts of tamoxifen in alphaMHC-MerCreMer mice induce a

DNA damage response, leading to heart failure and death. *Dis Model Mech* **6**:1459–1469. doi:10.1242/dmm.010447

Blader P, Plessy C, Strahle U. 2003. Multiple regulatory elements with spatially and temporally distinct activities control neurogenin1 expression in primary neurons of the zebrafish embryo. *Mech Dev* **120**:211–218.

Congote J. 2012. MEDX3DOM: MEDX3D for X3DOMProceedings of the 17th International Conference on 3D Web Technology, Web3D '12. New York, NY, USA: ACM. pp. 179–179. doi:10.1145/2338714.2338746

Davison JM, Akitake CM, Goll MG, Rhee JM, Gosse N, Baier H, Halpern ME, Leach SD, Parsons MJ. 2007. Transactivation from Gal4-VP16 transgenic insertions for tissue-specific cell labeling and ablation in zebrafish. *Dev Biol* **304**:811–824.

Dymecki SM, Ray RS, Kim JC. 2010. Mapping cell fate and function using recombinase-based intersectional strategies. *Methods Enzymol* **477**:183–213. doi:10.1016/S0076-6879(10)77011-7

Flanagan-Steet H, Fox MA, Meyer D, Sanes JR. 2005. Neuromuscular synapses can form in vivo by incorporation of initially aneural postsynaptic specializations. *Dev Camb Engl* **132**:4471–4481. doi:10.1242/dev.02044

Forster D, Arnold-Ammer I, Laurell E, Barker AJ, Fernandes AM, Finger-Baier K, Filosa A, Helmbrecht TO, Kolsch Y, Kuhn E, Robles E, Slanchev K, Thiele TR, Baier H, Kubo F. 2017. Genetic targeting and anatomical registration of neuronal populations in the zebrafish brain with a new set of BAC transgenic tools. *Sci Rep* **7**:5230. doi:10.1038/s41598-017-04657-x

Gohl DM, Silies MA, Gao XJ, Bhalerao S, Luongo FJ, Lin CC, Potter CJ, Clandinin TR. 2011. A versatile in vivo system for directed dissection of gene expression patterns. *Nat Methods* **8**:231–7.

Heffer A, Marquart GD, Aquilina-Beck A, Saleem N, Burgess HA, Dawid IB. 2017. Generation and characterization of Kctd15 mutations in zebrafish. *PloS One* **12**:e0189162. doi:10.1371/journal.pone.0189162

Horstick EJ, Jordan DC, Bergeron SA, Tabor KM, Serpe M, Feldman B, Burgess HA. 2014. Increased functional protein expression using nucleotide sequence features enriched in highly expressed genes in zebrafish **43**:e48. doi:10.1093/nar/gkv035

John NW, Aratow M, Couch J, Evestedt D, Hudson AD, Polys N, Puk RF, Ray A, Victor K, Wang Q. 2007. MedX3D: standards enabled desktop medical 3D. *Stud Health Technol Inform* **132**:189–194.

Kawakami K. 2007. Tol2: a versatile gene transfer vector in vertebrates. *Genome Biol* **8**:S7.

Marquart GD, Tabor KM, Brown M, Strykowski JL, Varshney GK, LaFave MC, Mueller T, Burgess SM, Higashijima S-I, Burgess HA. 2015. A 3D Searchable Database of Transgenic Zebrafish Gal4 and Cre Lines for Functional Neuroanatomy Studies. *Front Neural Circuits* **9**:78. doi:10.3389/fncir.2015.00078

Marquart GD, Tabor KM, Horstick EJ, Brown M, Geoca AK, Polys NF, Nogare DD, Burgess HA. 2017. High-precision registration between zebrafish brain atlases using symmetric diffeomorphic normalization. *GigaScience* **6**:1–15. doi:10.1093/gigascience/gix056

Obholzer N, Wolfson S, Trapani JG, Mo W, Nechiporuk A, Busch-Nentwich E, Seiler C, Sidi S, Söllner C, Duncan RN, Boehland A, Nicolson T. 2008. Vesicular Glutamate Transporter 3 Is Required for Synaptic Transmission in Zebrafish Hair Cells. *J Neurosci* **28**:2110–2118. doi:10.1523/jneurosci.5230-07.2008

Otsuna H, Hutcheson DA, Duncan RN, McPherson AD, Scoresby AN, Gaynes BF, Tong Z, Fujimoto E, Kwan KM, Chien CB, Dorsky RI. 2015. High-resolution analysis of central nervous system

expression patterns in zebrafish Gal4 enhancer-trap lines. *Dev Dyn* **244**:785–96. doi:10.1002/dvdy.24260

Pfeiffer BD, Ngo TT, Hibbard KL, Murphy C, Jenett A, Truman JW, Rubin GM. 2010. Refinement of tools for targeted gene expression in Drosophila. *Genetics* **186**:735–55. doi:10.1534/genetics.110.119917

Polys N, Wood A. 2012. New platforms for health hypermedia. *Issues Inf Syst* **13**:40–50.

Preibisch S, Saalfeld S, Tomancak P. 2009. Globally optimal stitching of tiled 3D microscopic image acquisitions. *Bioinformatics* **25**:1463–5. doi:10.1093/bioinformatics/btp184

Randlett O, Wee CL, Naumann EA, Nnaemeka O, Schoppik D, Fitzgerald JE, Portugues R, Lacoste AM, Riegler C, Engert F. 2015. Whole-brain activity mapping onto a zebrafish brain atlas. *Nat Methods* **12**:1039–46.

Satou C, Kimura Y, Hirata H, Suster ML, Kawakami K, Higashijima S. 2013. Transgenic tools to characterize neuronal properties of discrete populations of zebrafish neurons. *Development* **140**:3927–31. doi:10.1242/dev.099531

Schmidt-Supprian M, Rajewsky K. 2007. Vagaries of conditional gene targeting. *Nat Immunol* **8**:665–668. doi:10.1038/ni0707-665

Schneider CA, Rasband WS, Eliceiri KW. 2012. NIH Image to ImageJ: 25 years of image analysis. *Nat Methods* **9**:671–675. doi:10.1038/nmeth.2089

Scott EK, Baier H. 2009. The cellular architecture of the larval zebrafish tectum, as revealed by gal4 enhancer trap lines. *Front Neural Circuits* **3**:13. doi:10.3389/neuro.04.013.2009

Scott EK, Mason L, Arrenberg AB, Ziv L, Gosse NJ, Xiao T, Chi NC, Asakawa K, Kawakami K, Baier H. 2007. Targeting neural circuitry in zebrafish using GAL4 enhancer trapping. *Nat Methods* **4**:323–326.

Tabor KM, Smith TS, Brown M, Bergeron SA, Briggman KL, Burgess HA. 2018. Presynaptic Inhibition Selectively Gates Auditory Transmission to the Brainstem Startle Circuit. *Curr Biol CB* **28**:2527-2535.e8. doi:10.1016/j.cub.2018.06.020

Ting C-Y, Gu S, Guttikonda S, Lin T-Y, White BH, Lee C-H. 2011. Focusing transgene expression in Drosophila by coupling Gal4 with a novel split-LexA expression system. *Genetics* **188**:229–233. doi:10.1534/genetics.110.126193

Traver D, Paw BH, Poss KD, Penberthy WT, Lin S, Zon LI. 2003. Transplantation and in vivo imaging of multilineage engraftment in zebrafish bloodless mutants. *Nat Immunol* **4**:1238–1246. doi:10.1038/ni1007

Vladimirov N, Mu Y, Kawashima T, Bennett DV, Yang C-T, Looger LL, Keller PJ, Freeman J, Ahrens MB. 2014. Light-sheet functional imaging in fictively behaving zebrafish. *Nat Meth* **11**:883–4. doi:10.1038/nmeth.3040

Wada N, Javidan Y, Nelson S, Carney TJ, Kelsh RN, Schilling TF. 2005. Hedgehog signaling is required for cranial neural crest morphogenesis and chondrogenesis at the midline in the zebrafish skull. *Dev Camb Engl* **132**:3977–3988. doi:10.1242/dev.01943

Wei X, Potter CJ, Luo L, Shen K. 2012. Controlling gene expression with the Q repressible binary expression system in Caenorhabditis elegans. *Nat Methods* **9**:391–395. doi:10.1038/nmeth.1929

Xiao T, Roeser T, Staub W, Baier H. 2005. A GFP-based genetic screen reveals mutations that disrupt the architecture of the zebrafish retinotectal projection. *Dev Camb Engl* **132**:2955–2967. doi:10.1242/dev.01861

Zhu P, Fajardo O, Shum J, Schärer Y-PZ, Friedrich RW. 2012. High-resolution optical control of spatiotemporal neuronal activity patterns in zebrafish using a digital micromirror device. *Nat Protoc* **7**:1410. doi:10.1038/nprot.2012.072

363

	All lines (n=264)			Mapped (n=171)		
	Gal4	Cre	FP	Gal4	Cre	FP
Enhancer trap	138	65	5	96	15	4
Transgenic	20	0	36	20	0	36
Total	158	65	41	116	15	40

Table 1. Summary of transgenic lines in ZBB2

Total numbers of enhancer trap lines, and transgenic lines (made using promoter fragments from genes, or through BAC recombination), broken down by type: Gal4, Cre or fluorescent protein (FP). Right columns total the number of lines where genomic information driving the expression pattern is available. This information inherently exists for all transgenic lines (grey), and was derived through integration site mapping for enhancer trap lines.

Line	Vector	Integration site (zv10) chr:base(strand)	Expression	Publication
y371Et	REx2-SCP1-BGi-Cre-v2a-CFP	n/a	optic tectum, medulla oblongata (caudal), muscle	Marquart (2015)
y378Et	attp-REx2-SCP:BGi-Cre-v2a-CFP-attP	n/a	brain-specific, olfactory sensory neurons, pallium, subpallium, pineal complex, habenula	Marquart (2015)
y379Et	REx2-SCP1-BGi-Cre-v2a-CFP	6:58631990(-) Intron: sp7	brain-specific, pallium, anterior commissure, pineal complex, habenula, optic tectum, cerebellum, medulla (sparse)	Marquart (2015)
y380Et	REx2-SCP1-BGi-Cre-v2a-CFP	n/a	brain-specific, pallium,anterior commissure, habenula, optic tectum, cerebellum, medulla (rostral), Mauthner neurons	Marquart (2015)
y381Et	REx2-SCP1-BGi-Cre-v2a-CFP	12:8529347(-) 2550 bp from nrbf2b	brain-specific, cerebellum, medulla oblongata, Mauthner neurons	Marquart (2015)
y382Et	attp-REx2-SCP:BGi-Cre-v2a-CFP-attP	n/a	pallium, anterior commissure, optic tectum, tegmentum, cerebellum, medulla oblongata, muscle	Marquart (2015)
y383Et	attp-REx2-SCP:BGi-Cre-v2a-CFP-attP	7:40248497(+) 17414 bp from dnajb6b	brain-specific, pineal complex, tegmentum, cerebellum, medulla	Marquart (2015)
y384Et	REx2-SCP1-BGi-Cre-v2a-CFP	n/a	brain-specific, optic tectum, cerebellum	Marquart (2015)
y385Et	REx2-SCP1-BGi-Cre-v2a-CFP	n/a	pallium, habenula, optic tectum, jaw	Marquart (2015)
y445Et	REx2-SCP1:BGi-Cre-2a-Cer.zf3	3:32976789(-) Intron: rarab	pallium, habenula, medulla oblongata	This paper
y454Tg	eltC-REx2-SCP1:BGi-Cre-v2a-Cer	n/a	Rhombomere 3, Rhombomere 4, Rhombomere 5, Rhombomere 6	Tabor (2018)
y455Tg	[hoxb3a-dr16-gata2]-SCP1:BGi-Cre-v2a-Cer	n/a	Rhombomere 5, Rhombomere 6	Tabor (2018)
y456Et	REx2-SCP1:BGi-Cre-2a-Cer.zf3	n/a	medulla oblongata	This paper
y457Et	REx2-SCP1:BGi-Cre-2a-Cer.zf3	n/a	broad (possibly pan-neuronal)	This paper
y458Et	REx2-SCP1:BGi-Cre-2a-Cer.zf3	n/a	optic tectum, torus semicircularis, cerebellum, medulla oblongata	This paper
y459Et	REx2-SCP1:BGi-Cre-2a-Cer.zf3	9:34806701(-) 25351 bp from shox	habenula, optic chiasm, optic tectum, thalamus, hypothalamus	This paper
y461Tg	hoxb1a-SCP1:BGi-Cre-v2a-Cer	n/a	Rhombomere 4, Rhombomere 5, Rhombomere 6, Rhombomere 7	Tabor (2018)
y465Et	REx2-SCP1:BGi-Cre-2a-Cer	n/a	Rhombomere 3, Rhombomere 5	This paper
y466Tg	hoxa2-SCP1:BGi-Cre-v2a-Cer	n/a	Rhombomere 2	Tabor (2018)
y478Et	attP-REx2-SCP1:BGi-Cre-2a-Cer-attP	22:15873060(-) Exon: klf2a	olfactory epithelium, subpallium	This paper
y479Et	attP-REx2-SCP1:BGi-Cre-2a-Cer-attP	n/a	olfactory epithelium+bulb, pallium, optic tectum, thalamus, hypothalamus, valvula cerebelli, corpus cerebelli, trigeminal ganglion, vagal ganglion, muscle, intestine, heart, skin	This paper
y480Et	attP-REx2-SCP1:BGi-Cre-2a-Cer-attP	n/a	optic tectum, heart, muscle	This paper
y481Et	attP-REx2-SCP1:BGi-Cre-2a-Cer-attP	n/a	torus longitudinalis, pallium, cerebellum	This paper
y483Et	attP-REx2-SCP1:BGi-Cre-2a-Cer-attP	n/a	olfactory epithelium, olfactory bulb, subpallium, habenula, optic tectum (cellular layer), hypothalamus - diffuse nucleus, rhombomere 4 (dorsal cluster)	This paper
y484Et	REx2-SCP1:BGi-Cre-2a-Cer	8:15102079(+) Intron: bcar3	pallium	This paper
y485Et	REx2-SCP1:BGi-Cre-2a-Cer.zf3	n/a	pallium, medulla oblongata (Rhombomere 6 to spinal cord)	This paper
y486Et	REx2-SCP1:BGi-Cre-2a-Cer.zf3	n/a	cerebellum	This paper
y487Et	REx2-SCP1:BGi-Cre-2a-Cer.zf3	5:49022874(-)	pallium, cerebellum, medulla oblongata (dorsal area in rhombomere 2, rhombomere 3, rhombomere 4, rhombomere 5)	This paper
y488Et	REx2-SCP1:BGi-Cre-2a-Cer.zf3	25:14850800(+) 48091 bp from dnajc24	olfactory bulb, pallium, habenula, pretectum, thalamus, cerebellum, medulla oblongata	This paper
y489Et	REx2-SCP1:BGi-Cre-2a-Cer.zf3	n/a	olfactory epithelium, rhombomere 5	This paper
y490Et	REx2-SCP1:BGi-Cre-2a-Cer.zf3	19:31376385(-) 29736 bp from sync	rhombomere 5	This paper
y492Et	REx2-SCP1:BGi-Cre-2a-Cer.zf3	n/a	medulla oblongata	This paper
y493Et	REx2-SCP1:BGi-Cre-2a-Cer.zf3	1:45228474(-) Intron: pnpla6	retinotectal tract, olfactory epithelium	This paper
y494Et	REx2-SCP1:BGi-Cre-2a-Cer.zf3	n/a	tegmentum	This paper
y495Et	REx2-SCP1:BGi-Cre-2a-Cer.zf3	22:30270429(-) Intron: add3a	medulla oblongata, radial glia (optic tectum)	This paper
y519Et	REx2-SCP1:BGi-Cre-2a-Cer	n/a	optic tectum	This paper
y520Et	REx2-SCP1:BGi-Cre-2a-Cer	n/a	pallium, cerebellum	This paper
y521Et	REx2-SCP1:BGi-Cre-2a-Cer.zf3	14:16528387(+) Intron: limch1b	medulla oblongata (caudal area)	This paper
y523Et	REx2-SCP1:BGi-Cre-2a-Cer.zf3	n/a	Mauthner cells, Rhombomere 6	This paper
y524Et	REx2-SCP1:BGi-Cre-2a-Cer	n/a	otic vesicle hair cells	This paper
y526Et	REx2-SCP1:BGi-Cre-2a-Cer.zf3	5:38414082(-) Intron: fras1	optic tectum, habenula	This paper
y528Et	REx2-SCP1:BGi-Cre-2a-Cer.zf3	6:55647153(+)	habenula (including fasciculus retroflexus), optic tectum, trigeminal ganglion	This paper
y541Et	REx2-SCP1:BGi-Cre-2a-Cer.zf3	n/a	pallium, optic tectum, cerebellum	This paper
y542Et	REx2-SCP1:BGi-Cre-2a-Cer.zf3	n/a	Rhombomere 6	This paper
y543Et	REx2-SCP1:BGi-Cre-2a-Cer.zf3	n/a	olfactory epithelium, subpallium, thalamus, pretectum, optic tectum, torus semicircularis, hypothalamus	This paper

y544Et	REx2-SCP1:BGi-Cre-2a-Cer.zf3	n/a	rhombomere 5, jaw	This paper
y545Et	REx2-SCP1:BGi-Cre-2a-Cer.zf3	n/a	Mauthner cells	This paper
y546Et	REx2-SCP1:BGi-Cre-2a-Cer.zf3	n/a	olfactory bulb, pallium, subpallium, habenula, pineal, optic tectum, thalamus, corpus cerebelli	This paper
y547Et	REx2-SCP1:BGi-Cre	n/a	subpallium, medulla oblongata (dorsal)	This paper
y548Et	REx2-SCP1:BGi-Cre	n/a	pallium, tegmentum, rhombomere 1, retina	This paper
y549Et	REx2-SCP1:BGi-Cre	n/a	rhombomere 2, rhombomere 4	This paper
y550Et	REx2-SCP1:BGi-Cre	n/a	olfactory bulb, pallium	This paper
y551Et	REx2-SCP1:BGi-Cre-2a-Cer.zf3	n/a	optic tectum (caudal domain)	This paper
y552Et	REx2-SCP1:BGi-Cre-2a-Cer.zf3	n/a	subpallium, telencephalic migrated area M4, hypothalamus - rostral zone, migrated posterior tubercular area M2, hypothalamus - intermediate zone	This paper
y554Et	REx2-SCP1:BGi-Cre-2a-Cer.zf3	n/a	medulla oblongata (lateral longitudinal column)	This paper
y555Et	REx2-SCP1:BGi-Cre	n/a	olfactory bulb, pallium, corpus cerebelli, optic tectum - stratum periventriculare, medulla oblongata (dorsal region)	This paper
y556Et	REx2-SCP1:BGi-Cre	n/a	olfactory bulb, pallium, optic tectum, optic tract, torus semicircularis, corpus cerebelli, medulla oblongata	This paper
y557Et	REx2-SCP1:BGi-Cre	n/a	thalamus, optic tract, optic tectum, valvula cerebelli, corpus cerebelli, medulla oblongata (caudal)	This paper
y558Et	REx2-SCP1:BGi-Cre-2a-Cer.zf3	n/a	olfactory bulb, pallium, optic tectum, torus semicircularis, cerebellum, medulla oblongata	This paper
y559Et	REx2-SCP1:BGi-Cre	n/a	Rhombomere 5 (dorsal domain), Rhombomere 6 (longitudinal column)	This paper
y568Et	REx2-SCP1:BGi-Cre-2a-Cer.zf3	n/a	ventral thalamus, Rhombomere 4, Rhombomere 5	This paper
y569Et	REx2-SCP1:BGi-Cre	n/a	olfactory epithelium, valvular cerebelli	This paper
y570Et	REx2-SCP1:BGi-Cre	n/a	Rhombomere 2, Rhombomere 3	This paper
y571Et	R2R6-hoxa2-CNE-SCP1:BGi-Cre-2a-Cer	n/a	Rhombomere 2, Rhombomere 6	This paper
y574Et	REx2-SCP1:BGi-Cre	n/a	olfactory bulb, pallium, habenula, optic tectum, griseum tectale, corpus cerebelli, medulla oblongata	This paper

Table S1. Summary of ZBB2 Cre lines
Integration site given in zv10 coordinates, transgene orientation indicated in brackets. Integration sites inside genes are annotated, or nearest Refseq gene (if within 50kb) indicated.

Line	Vector	Integration site (zv9/10) chr:base(strand)	Expression	Publication
y234Et	SCP1:Gal4ff	10:28607866(+)z9 51288 bp from ints2	trigeminal ganglion, pineal complex (projection neurons), medulla (caudal), retina, spinal cord, weak heart, weak muscle, axial vasculature (intersegmental vessels)	Yokogawa J Neurosci (2012)
y236Et	REx2-cfos:kGal4ff	14:32488427(-)z9 343 bp from mmgt1	brain-specific, olfactory sensory neurons, hypothalamus - caudal zone, retina, spinal cord	Bergeron Front Neural Circuits (2012)
y237Et	REx2-cfos:kGal4ff	25:19691130(-)z9 176 bp from hapln3	brain-specific, optic tectum, vagal region, spinal cord	Bergeron Front Neural Circuits (2012)
y240Et	cfos:kGal4ff	22:18778916(+)z9 8555 bp from cirbp	olfactory sensory neurons, olfactory bulb, pineal complex, posterior tuberculum, rhombomere 3, rhombomere 5, pLLg, lateral line, retina, spinal cord, strong lens, weak heart, weak notochord, fast muscle, median fin fold, punctate cells on yolk and extension, integument	Marquart Front Neural Circuits (2015)
y241Et	REx2-SCP1:kGal4ff	1:619473(-)z9 First intron: dusp27	hypothalamus - caudal zone, retinal ganglion cells, retinotectal tract, optic tectum, fast muscle, weak heart	Fero Dis Mod Mech (2013)
y242Et	REx2-SCP1:Gal4	16:11407834(+)z10 Intron: znf574	olfactory bulb, subpallium, habenula, pineal, pretectum, locus coeruleus, medulla oblongata, retina, spinal cord (radial glia), motor neurons, slow muscle (weak), integument (strong in patch dorsal to rhombomere 5), habenula, heart (weak)	This paper
y244Et	REx2-SCP1:kGal4ff	n/a	subpallium, habenula (lateral region;plus fasciculus retroflexus terminating below median raphe), band of neurons from posterior tuberculum to hypothalamus (intermediate), hypothalamus - caudal zone, retina, spinal cord strong fast muscle, liver	Bergeron Front Neural Circuits (2012)
y245Et	SCP1:Gal4ff	8:41559388(-)z9 161 bp from msi1	brain-specific, habenula (left;medial region), periventricular cells, pineal complex, medulla oblongata (dorsal;caudal), retina, spinal cord, broad moderate intensity brain expression	Marquart Front Neural Circuits (2015)
y249Et	REx2-SCP1:kGal4ff	Un_KN150107v1:41677(?)z10 no adjacent genes	brain-specific, olfactory sensory neurons, subpallium (lateral/ventral), pineal complex, Nuc MLF, posterior commissure, hypothalamus - caudal zone, aLLg, pLLg, habenula (left), retinotectal tract, otic vesicle cristae, cerebellum, medulla (anterior and longitudinal stripes), spinal cord	Marquart Front Neural Circuits (2015)
y252Et	REx2-SCP1:kGal4ff	5:71036701(-)z9 20796 bp from gsx1	posterior tuberculum, griseum tectale, optic tectum, hypothalamus, cerebellum, medulla (longitudinal stripe; hindbrain commissures), retina, spinal cord	Begeron Mol Psych (2015)
y255Et	REx2-cfos:kGal4ff	4:8078727(+)z9 First intron: scube1	brain-specific, posterior tuberculum, medulla (caudal)	Marquart Front Neural Circuits (2015)
y256Et	SCP1:Gal4ff	18:39202322(-)z9 Intron: pglyrp5	statoacoustic ganglion (selective;strong), retina, spinal cord	Marquart Front Neural Circuits (2015)
y264Et	SCP1:Gal4ff	17:49286618(+)z9 Exon: TIAM2(1of2)	olfactory sensory neurons, pallium, subpallium, torus longitudinalis, Mauthner neurons, reticulospinal neurons, cerebellum (eminentia granularis), weak intestine, weak heart, weak muscle	Tabor J Neurophysiol (2014)
y265Et	SCP1:Gal4ff	1:54550186(+)z9 Exon: rhou(1of3)	olfactory epithelium, subpallium, pineal, thalamus, tegmentum, medulla oblongata (longitudinal stripes), retina, ocular muscle, motor neurons, esophagus	This paper
y269Et	REx2-cfos:kGal4ff	20:32151328(+)z9 1555 bp from grm1a	brain-specific, pallium (central zone), optic tectum, hypothalamus - caudal zone, retinotectal tract, medulla (longitudinal stripe), aLLg, pLLg, spinal cord	Tabor J Neurophysiol (2014)
y270Et	REx2-cfos:kGal4ff	10:40378086(+)z9 Intron: igsf5a	brain-specific, pallium (dorso-medial telencephalon), pineal (selective), reticulospinal neurons (small subset), medulla (caudal; ventral), motor neurons, retina, spinal cord	Tabor J Neurophysiol (2014)
y271Et	SCP1:kGal4ff	n/a	brain (broad, strong), spinal cord (broad), heart (weak), muscle (weak), notochord (weak)	Horstick EJ Nuc Ac Res (2015)
y274Et	SCP1:Gal4ff	5:51191297(-)z9	brain (broad), spinal cord (broad), notochord, heart, slow muscle, fins, ocular muscle	This paper
y275Et	REx2-SCP1:kGal4ff	18:21417110(-)z10 2631 bp from necab2	olfactory sensory neurons, subpallium, preoptic region, pretectum, optic tectum, tegmentum, cerebellar plate, cerebellum (eminentia granularis), torus longitudinalis, torus semicircularis, hypothalamus, medulla (caudal), retina, motor neurons, punctate cells on yolk	Marquart Front Neural Circuits (2015)
y279Et	REx2-SCP1:kGal4ff	n/a	subpallium, preoptic region, habenula (left;medial region), ventral thalamus, hypothalamus - caudal zone, trigeminal ganglion, statoacoustic ganglion, aLLg, pLLg, lateral line, optic tectum (radial glia), reticulospinal neurons, medulla (medial cluster), retina, spinal cord	Marquart Front Neural Circuits (2015)
y293Et	tphR:Gal4ff	19:29918823(-)z9 First intron: fndc5b	pineal complex, tegmentum, posterior commissure, dorsal raphe, medulla (two clusters: antero-lateral;dorso-medial), retina, spinal cord, notochord	Marquart Front Neural Circuits (2015)
y294Et	tphR:Gal4ff	22:24988502(+)z9 2610 bp from C22H1orf53	brain-specific, olfactory sensory neurons, pallium, subpallium, pineal complex, habenula (plus fasciculus retroflexus), thalamus, posterior tuberculum, dorsal raphe, optic tectum, tegmentum, torus semicircularis, medulla oblongata, hindbrain commissures, retina, spinal cord (ventral)	Marquart Front Neural Circuits (2015)
y295Et	cfos:Gal4ff	n/a	medulla (rhombomere 4;rhombomere 6), spinal cord (primary motor neurons), heart	Marquart Front Neural Circuits (2015)
y296Et	cfos:Gal4ff	22:9916974(-)z9 42 bp from si:ch211-236g6.1	olfactory sensory neurons (selective), hypothalamus - caudal zone, pituitary (pars anterior), neuromasts (hair cells;mantle cells;glia), integument (weak), punctate cells on integument, branchial arches	Marquart Front Neural Circuits (2015)
y297Et	cfos:Gal4ff	11:12425507(+)z10 Intron: zgc:174353	brain-specific, trigeminal, pLLg, lateral line, medulla (ventral longitudinal stripe), pituitary (pars intermedia), retina, motor neurons	Marquart Front Neural Circuits (2015)
y298Et	tphR:Gal4ff	9:5189792(+)z9 12901 bp from CU207353.2	brain-specific, pallium (small rostral cluster), pineal complex, habenula, optic tectum, pLLg, cerebellum, medulla oblongata, retina, spinal cord	Marquart Front Neural Circuits (2015)
y299Et	cfos:kGal4ff	10:39345827(+)z9 10634 bp from WSCD1(2of3)	olfactory bulb, pallium, tegmentum, medulla oblongata, hypothalamus - caudal zone, primary motor neurons (strong), weak heart	Marquart Front Neural Circuits (2015)
y300Et	cfos:kGal4ff	24:25072485(-)z9 1191 bp from bhlhe22	brain-specific, pallium, retinotectal tract, posterior tuberculum, preglomerula complex (M2), optic tectum (neuropil), hypothalamus, cerebellum (cerebellar plate), medulla (anterior cluster; caudal medial longitudinal stripe), retina (retinal ganglion cells), spinal cord	Marquart Front Neural Circuits (2015)
y301Et	cfos:Gal4ff	7:39422607(+)z9 55232 bp from cebpa	medulla (caudal), retina (photoreceptor layer), intestine, blood, weak heart, liver	Marquart Front Neural Circuits (2015)
y302Et	cfos:kGal4ff	20:31771236(+)z9 621 bp from stxbp5a	habenula (medial region), tegmentum, posterior tuberculum, inferior olive, retina, notochord, integument (patches above medulla oblongata and around heart), weak heart, weak muscle	Marquart Front Neural Circuits (2015)

y303Et	cfos:kGal4ff	n/a	posterior tuberculum, trigeminal ganglion, medulla (small cluster), punctate cells on yolk, weak heart, muscle	Marquart Front Neural Circuits (2015)
y304Et	cfos:kGal4ff	16:7507246(-)z9 43295 bp from CMTM8(1of2)	habenula, pretectum, ventral thalamus, optic tectum (cells; fibres from tectum descending into hindbrain), torus longitudinalis, hypothalamus - caudal zone, retina, spinal cord, weak muscle, strong heart	Marquart Front Neural Circuits (2015)
y305Et	cfos:kGal4ff	n/a	pallium, subpallium, habenula, cerebellum (eminentia granularis), retina, spinal cord, caudal tip of tail, weak muscle	Marquart Front Neural Circuits (2015)
y306Et	REx2-SCP1:kGal4ff	5:3818536(+)z10 3' UTR: si:ch211-283g2.1	brain-specific, preoptic region (selective)	Marquart Front Neural Circuits (2015)
y307Et	REx2-SCP1:kGal4ff	15:40794745(-)z9 Exon: farsb	medulla (three discrete clusters: anterior; in r4; longitudinal stripe), retina, spinal cord, intestine	Marquart Front Neural Circuits (2015)
y308Et	tphR:Gal4ff	19:47897584(+)z10 1465 bp from tfap2e	brain-specific, olfactory sensory neurons, olfactory bulb, optic tectum, dorsal raphe, medulla (rostral)	Marquart Front Neural Circuits (2015)
y309Et	REx2-SCP1:kGal4ff	n/a	posterior commissure, Nuc MLF, aLLg, pLLg, retina, weak blood, cells on intestine	Marquart Front Neural Circuits (2015)
y310Et	REx2-SCP1:kGal4ff	1:23474284(-)z9 17479 bp from si:ch211-188p14.8	brain-specific, pineal complex, posterior tuberculum, hypothalamus - caudal zone, optic tectum (sparse)	Marquart Front Neural Circuits (2015)
y311Et	REx2-SCP1:kGal4ff	n/a	pallium, subpallium, anterior commissure, preoptic region, thalamic eminence, pineal complex, habenula, optic tectum, inferior olive, cerebellum, habenula, retina, spinal cord, intestine, jaw, weak heart	Marquart Front Neural Circuits (2015)
y312Et	REx2-SCP1:kGal4ff	1:21429774(-)z9 Intron: anxa5b	brain-specific, olfactory sensory neurons (selective), olfactoy bulb, subpallium, retina, spinal cord	Marquart Front Neural Circuits (2015)
y313Et	REx2-SCP1:kGal4ff	15:52608(+)z9 1696 bp from si:zfos-411a11.2	brain-specific, posterior tuberculum, Nuc MLF, medulla (caudal), retina, spinal cord	Marquart Front Neural Circuits (2015)
y314Et	SCP1:Gal4ff	14:31129791(+)z9 12733 bp from asah1a	medulla (rostral; caudal ventro-medial clusters), retina (photoreceptor layer), spinal cord, weak heart, weak muscle	Marquart Front Neural Circuits (2015)
y315Et	cfos:Gal4ff	n/a	medulla (caudal), spinal cord (strong; broad;motor neurons), strong heart	Marquart Front Neural Circuits (2015)
y316Et	cfos:Gal4ff	3:51530714(-)z9 95609 bp from AL929327.3	olfactory sensory neurons (discrete rostro-medial cluster), retinotectal tract, spinal cord, weak notochord, weak pancreas	Marquart Front Neural Circuits (2015)
y317Et	SCP1:Gal4ff	10:6763413(-)z9 Exon: snx24	posterior tuberculum, trigeminal ganglion, pLLg, reticulospinal neurons, spinal cord, heart, muscle	Marquart Front Neural Circuits (2015)
y318Et	REx2-SCP1:kGal4ff	7:47621609(-)z9 Intron: zgc:162297	cerebellum (selective; cerebellar plate; eminentia granularis), pLLg, cranial sensory ganglia, spinal cord, intestine	Marquart Front Neural Circuits (2015)
y319Et	REx2-SCP1:kGal4ff	1:40177687(-)z9 Intron: dctd	habenula (strong lateral;plus fasciculus retroflexus to below median raphe), Nuc MLF, statoacoustic ganglion (restricted portion with dorsal projection), retina, spinal cord, weak heart	Marquart Front Neural Circuits (2015)
y320Et	REx2-SCP1:kGal4ff	19:28217946(-)z10 28649 bp from papd7	olfactory sensory neurons, pallium, preoptic region, posterior tuberculum, hypothalamus, aLLg, pLLg, strong cranial sensory ganglia (plus plexus in medulla), inferior olive, retina, spinal cord, swim bladder, lens	Marquart Front Neural Circuits (2015)
y321Et	REx2-SCP1:kGal4ff	2:11002513(+)z9 1032 bp from lhx8a	brain-specific, subpallium, preoptic region, rostral hypothalamus, posterior tuberculum	Marquart Front Neural Circuits (2015)
y322Et	REx2-SCP1:kGal4ff	19:44346108(-)z9 Intron: clasp2	brain-specific, olfactory sensory neurons, medulla (small rostral cluster),retina, spinal cord	Marquart Front Neural Circuits (2015)
y323Et	REx2-SCP1:kGal4ff	7:54648943(-)z9 Exon: fgf3	subpallium, posterior tuberculum, hypothalamus - caudal zone, cerebellum, rhombomere 4, otic vesicle maculae, retina, heart, slow muscle	Marquart Front Neural Circuits (2015)
y324Et	cfos:Gal4ff	12:40486192(-)z9 Intron: si:dkey-239b22.1	brain-specific, medulla (ventro-medial cluster of neurons), retina, spinal cord	Marquart Front Neural Circuits (2015)
y325Et	SCP1:Gal4ff	2:22371041(+)z10 Intron: tox	olfactory sensory neurons, posterior tuberculum, optic tectum, pituitary, reticulospinal neurons, trigeminal ganglion, aLLg, pLLg, neuromasts (strong), medulla (caudal/dorsal and longitudinal stripe), otic vesicle maculae, retinotectal tract, spinal cord, endocrine pancreas, fast muscle	Marquart Front Neural Circuits (2015)
y326Et	cfos:kGal4ff	3:50931110(+)z9 25527 bp from TRIM35(3of41)	brain-specific, reticulospinal neuron (selective; two bilateral pairs), pituitary (pars anterior)	Marquart Front Neural Circuits (2015)
y327Et	REx2-cfos:kGal4ff	3:10432998(-)z9 34994 bp from si:ch73-208g21.1	brain-specific, hypothalamus - rostral zone (selective), subpallium, posterior tuberculum, medulla (medio-lateral cluster), pLLg, neuromasts	Marquart Front Neural Circuits (2015)
y328Et	REx2-cfos:kGal4ff	16:29654676(-)z9 Exon: erp44	brain-specific, subpallium, habenula (plus fasciculus retroflexus), torus longitudinalis, medulla (dorsal caudal), floorplate (brain and spinal cord), retina	Marquart Front Neural Circuits (2015)
y329Et	REx2-cfos:kGal4ff	2:18388917(+)z9 13027 bp from 5S-rRNA	subpallium, thalamic eminence, ventral thalamus, posterior tuberculum, hypothalamus - caudal zone, optic tectum, vagal region, motor neurons, retina, punctate cells on yolk	Marquart Front Neural Circuits (2015)
y330Et	cfos:kGal4ff	6:4283166(-)z9 7609 bp from RBM26	habenula (strong; plus fasciculus retroflexus to interpeduncular nucleus), inferior olive, trigeminal ganglion, aLLg, statoacoustic ganglion, pLLg, muscle, pronephric ducts, retina, spinal cord	Marquart Front Neural Circuits (2015)
y331Et	REx2-cfos:kGal4ff	n/a	brain-specific, pallium, optic tectum (neuropil), medulla (clusters), reticulospinal neurons, retina, spinal cord	Marquart Front Neural Circuits (2015)
y332Et	REx2-cfos:kGal4ff	24:27249324(+)z9 Intron: slc7a14b	brain-specific, habenula (right;medial;plus fasciculus retroflexus), hypothalamus - caudal zone, otic maculae, retina, spinal cord	Marquart Front Neural Circuits (2015)
y333Et	REx2-cfos:kGal4ff	2:54258467(+)z10 9673 bp from ctnnbl1	brain-specific, hypothalamus -caudal zone (selective), medulla oblongata, spinal cord	Marquart Front Neural Circuits (2015)

y334Et	REx2-cfos:kGal4ff	5:57921796(+)z10 Intron: pou2f3	brain-specific, cerebellum, medulla (discrete clusters), reticulospinal neurons, retina, spinal cord	Marquart Front Neural Circuits (2015)
y336Et	REx2-SCP1:kGal4ff	22:22987582(+)z10 Intron: ptprc	optic tectum, retinotectal tract (strong), hypothalamus - caudal zone, pituitary (strong; pars intermedia), medulla (caudal/ventral), retina, spinal cord, pancreas	Marquart Front Neural Circuits (2015)
y337Et	REx2-cfos:kGal4ff	2:10272050(+)z9 Intron: CCDC18 (1 of 2)	brain-specific, pLLg, spinal cord (floorplate)	Marquart Front Neural Circuits (2015)
y338Et	cfos:kGal4ff	n/a	brain-specific, pretectum (migrated area), optic tectum (anterior/lateral), medulla (rostral), neuromasts (sparse), retina	Marquart Front Neural Circuits (2015)
y339Et	REx2-cfos:kGal4ff	n/a	brain-specific, hypothalamus - rostral zone (selective), pallium, retina	Marquart Front Neural Circuits (2015)
y341Et	REx2-cfos:kGal4ff	14:31278235(-)z10 398 bp from mmgt1	brain-specific, hypothalamus - caudal zone (selective), retina, spinal cord	Marquart Front Neural Circuits (2015)
y342Et	REx2-cfos:kGal4ff	21:44291658(+)z9 10743 bp from si:ch211-25g7.3	brain-specific, medulla (caudal cluster), pLLG, retina, spinal cord	Marquart Front Neural Circuits (2015)
y345Et	REx2-cfos:kGal4ff	9:10031215(+)z9 First intron: fstl1b	brain-specific, subpallium, reticulospinal neurons, medulla (caudal cluster), retina, spinal cord	Marquart Front Neural Circuits (2015)
y347Et	REx2-SCP1:kGal4ff	25:654264(-)z9 211 bp from znf609a	hypothalamus - caudal zone (selective), medulla oblongata, floorplate, retina	Marquart Front Neural Circuits (2015)
y348Et	REx2-SCP1:kGal4ff	3:7519484(-)z9 1180 bp from BX000701.2	olfactory sensory neurons, posterior tuberculum, tegmentum, trigeminal ganglion, reticulospinal neurons, retina, spinal cord	This paper
y350Et	SCP1:Gal4ff	23:242920(-)z9 First intron: PDZD4	Habenula (right), thalamus, hypothalamus - rostral zone, tegmentum, trigeminal motor neurons - posterior, medulla oblongata	Marquart Front Neural Circuits (2015)
y351Et	SCP1:Gal4ff	8:26512923(+)z9 Intron: sema3ga	olfactory sensory neurons, Nuc MLF, posterior commissure, medulla (dorsal/caudal), hindbrain commissures, retina, spinal cord, fin	Marquart Front Neural Circuits (2015)
y352Et	SCP1:Gal4ff	9:22412697(+)z10 Intron: crygm2d8	medulla oblongata (small lateral cluster in ~rhombomere 6), lens, retina	Marquart Front Neural Circuits (2015)
y353Et	cfos:kGal4ff	14:6556477(+)z10 68318 bp from si:ch211-266k2.1	pretectum, hypothalamus - caudal zone, medulla (discrete clusters), pLLg, strong lens, esophagus/pharynx, jaw, ocular muscle, fins	Marquart Front Neural Circuits (2015)
y354Et	REx2-SCP1:kGal4ff	n/a	retinotectal tract (selective; additional retinal arborization fields), medulla oblongata, spinal cord, strong heart, intestine	Marquart Front Neural Circuits (2015)
y355Et	tphR:Gal4ff	7:47999107(-)z9 First intron: znf536	dorsal raphe, medulla oblongata (two clusters), otic vesicle cristae, lateral line (glia), retina, spinal cord, weak heart, weak notochord, weak ocular muscle	Marquart Front Neural Circuits (2015)
y356Et	SCP1:Gal4ff	n/a	cerebellum (cerebellar plate), optic tectum (radial glia), retina, spinal cord, heart, fast muscle, integument, yolk, fin, branchial arches	Marquart Front Neural Circuits (2015)
y357Et	REx2-SCP1:kGal4ff	n/a	pallium, subpallium, pineal complex, dorsal thalamus, ventral thalamus, optic tectum, tegmentum, inferior olive, cranial sensory ganglia, pLLg, lateral line (innervation of neuromasts), retina, spinal cord, weak muscle, punctate cells on pectoral fin, median fin fold	Marquart Front Neural Circuits (2015)
y358Et	REx2-cfos:kGal4ff	n/a	vagal region, cranial sensory ganglia, motor neurons, retina, weak muscle, floorplate, swimbladder	Marquart Front Neural Circuits (2015)
y359Et	-3.0dbh:Gal4ff	n/a	brain-specific, trigeminal motor neurons - anterior	Marquart Front Neural Circuits (2015)
y364Et	SCP1:Gal4ff	14:18043955(+)z10 321736 bp from slitrk4	pallium, radial glia (telencephalon/diencephalon), pineal complex, hypothalamus - caudal zone, pLLg, lateral line, neuromasts (head and trunk), medulla (radial glia), retina, spinal cord, muscle, integument (weak)	Marquart Front Neural Circuits (2015)
y365Et	cfos:Gal4ff	18:24119849(+)z10 231334 bp from nr2f2	broadly expressed, thalamus, ventral midbrain, cerebellum, medulla oblongata, motor neurons, retina, weak heart, weak vasculature	Marquart Front Neural Circuits (2015)
y372Et	SCP1:Gal4ff	1:46762378(-)z9 Exon: atp11a	hypothalamus - rostral zone, reticulospinal neurons, otic vesicle cristae, trigeminal ganglion, aLLg, pLLg, retina, spinal cord, fast muscle, heart	Marquart Front Neural Circuits (2015)
y373Et	REx2-SCP1:kGal4ff	22:20316172(-)z9 First intron: celf5a	pallium, subpallium, habenula, optic tectum, torus longitudinalis, torus semicircularis, inferior olive, weak motor neurons, weak muscle, cells on intestine	Marquart Front Neural Circuits (2015)
y375Et	SCP1:Gal4ff	7:43085823(+)z10 Intron: BX005003.1	subpallium, pineal complex, habenula (lateral;fasciculus retroflexus to below medial raphe), ventral thalamus, pituitary, medulla oblongata, Nuc MLF, medulla, motor neurons, retina, spinal cord, strong heart, weak ventral fin	Marquart Front Neural Circuits (2015)
y387Et	tph2:Gal4ff	24:40333322(-)z9 3501 bp from nog2	olfactory bulb, subpallium, habenula, medulla oblongata, dorsal raphe, retina, spinal cord, muscle (including ocular muscle), fin, notochord	This paper
y388Et	SCP1:Gal4ff	7:65387548(+)z9 19959 bp from lypla1	vasculature (intersegmental vessels)	Marquart Front Neural Circuits (2015)
y393Et	cfos:Gal4ff	19:40581722(+)z9 First intron: BAI2	olfactory sensory neurons, pallium, subpallium, pineal, habenula (lateral), trigeminal ganglion, hypothalamus, pituitary, otic vesicle maculae (posterior), retina, spinal cord, floorplate, fast muscle	Marquart Front Neural Circuits (2015)
y394Et	cfos:Gal4ff	24:13365039(+)z9 Intron: kcnb2(2of2)	olfactory bulb, subpallium, posterior tuberculum, facial octavolateralis motor neurons, vagus motor neurons, inferior olive, motor neurons, ocular muscle, strong pectoral fin, yolk extension, weak slow muscle	This paper
y396Et	SCP1:Gal4ff	10:172834(-)z9 First intron: pigp	olfactory bulb, medulla oblongata, aLLg, pLLg, branchial arches, endocrine pancreas, neuromasts, retina, spinal cord	Marquart Frontiers (2015)
y397Et	SCP1:Gal4ff	10:8107827(-)z9 First intron: Talin1	aLLg, pLLg, lateral line, blood, fin, notochord (strong), muscle (weak)	Marquart Front Neural Circuits (2015)

y401Et	cfos:Gal4ff	10:17306571(-)z9 17614 bp from stoml2	optic tectum (radial glia), ventricles, olfactory epithelium, muscle (weak), heart (weak), yolk	Marquart Front Neural Circuits (2015)
y405Et	SCP1:Gal4ff	15:38142438(+)z9 Intron: Robo2	olfactory epithelium, preoptic area, trigeminal ganglion, locus coeruleus, optic tectum, medulla oblongata, retina, spinal cord, muscle	Marquart Front Neural Circuits (2015)
y407Et	SCP1:Gal4ff	3:43696002(+)z9 Exon: psmg3	subpallium, telencephalic migrated area M4, hypothalamus, optic tectum (neuropil), diencephalon, tegmentum, neuromasts (head, trunk), pLLg, weak muscle, endocrine pancreas, median fin fold, medulla (caudal dorso-lateral)	Marquart Frontiers (2015)
y412Et	cfos:Gal4ff	11:29785662(-)z9 Intron: igsf21a	subpallium, tegmentum, eminentia granularis, corpus cerebelli, medulla oblongata, heart	This paper
y416Et	cfos:Gal4ff	15:17514660(-)z9 First intron: ncam1b	pineal complex, hypothalamus - rostral zone, optic tectum (neuropil), vagal ganglion, aLLg, pLLg, lateral line, cranial sensory ganglia, dorsal root ganglia, retina, spinal cord, intestine, weak notochord, weak ventral fast muscle	This paper
y417Et	REx2-SCP1:Gal4ff	24:4752371(+)z9 82747 bp from cpb1	olfactory epithelium, telencephalon (ventral midline), lateral habenula, optic tectum, medulla oblongata, vagal ganglion, heart (strong), intestine (strong), somite boundaries, neuromasts (head only)	Marquart Front Neural Circuits (2015)
y420Et	REx2-cfos:Gal4ff	11:25874207(+)z9 First intron: sulf2a	olfactory sensory neurons, hypothalamus - rostral zone, posterior tuberculum, tegmentum, medulla oblongata (rostral nuclei), aLLg, pLLg, lateral line, neuromasts, spinal cord, floorplate, blood	Marquart Frontiers (2015)
y421Et	REx2-cfos:Gal4	12:26823958(-)z9 2210 bp from hcar1-4	pallium, thalamus, posterior tuberculum, hypothalamus - rostral zone, meninges, retina, spinal cord, yolk, muscle, notochord, fin, jaw	This paper
y423Et	REx2-cfos:Gal4ff	20:15525164(-)z9 9667 bp from si:dkey-86e18.4	optic tectum (neuropil), medulla oblongata (several clusters), vagus motor neurons, trigeminal ganglion, aLLg, pLLg, vagal ganglion, retina, spinal cord, endocrine pancreas, notochord	Marquart Front Neural Circuits (2015)
y425Et	REx2-cfos:Gal4ff	13:46570157(+)z9 2637 bp from bsdc1	olfactory bulb, hypothalamus, motor neurons (weak), spinal cord, heart (weak), floorplate	Marquart Front Neural Circuits (2015)
y433Et	cfos:kGal4ff	16:4477730(+)z10 Intron: vegfaa	tegmentum, reticulospinal neurons, fast muscle (strong), pectoral fins	This paper
y436Et	cfos:Gal4ff	n/a	olfactory sensory neurons, retina, lens, posterior tuberculum, pronephric tubules, caudal fin rays, notochord (weak), notochord, muscle, spinal cord	This paper
y441Et	cfos:Gal4ff	12:25705427(-)z10 Intron: epas1a	pineal projection neurons, hypothalamus, vagal ganglion, slow muscle (weak), heart, skin, retina, spinal cord	This paper
y444Et	SCP1:Gal4ff	n/a	pituitary, reticulospinal, notochord, retina, spinal cord	This paper
y467Et	tph2:Gal4ff	n/a	subpallium, hypothalamus - caudal zone, tegmentum, dorsal raphe, Rhombomere 3, Rhombomere 5, endocrine pancreas, motor neurons (weak), heart (weak)	This paper
y468Et	cfos:Gal4ff	n/a	olfactory epithelium, pallium, hypothalamus, cranial sensory ganglia, aLLg, vagal ganglion, intestine, retinal, spinal cord	This paper
y469Et	cfos:Gal4ff	14:281181013(+)z10 Intron: stag2b	retinotectal tract, medulla oblongata (floorplate)	This paper
y470Et	REx2-SCP1:Gal4ff	n/a	pineal complex, subpallium, optic tectum (weak), posterior tuberculum, hypothalamus - caudal zone, anterior macula, middle crista, ocular muscle, integument	This paper
y471Et	REx2-SCP1:Gal4ff	n/a	subpallium, preoptic area, hypothalamus, oculomotor nucleus, interpeduncular nucleus tegmentum, dorsal raphe, medulla oblongata (R1, caudal lateral area), motor neurons, intestine, muscle (weak), iridophores, pectoral fins (strong), medial fin fold (caudal), blood (weak)	This paper
y472Et	REx2-SCP1:Gal4ff	n/a	olfactory epithelium, preoptic area, habenula, hypothalamus, tegmentum, medulla oblongata, intestine	This paper
y473Et	cfos:Gal4ff	n/a	pituitary, tegmentum, medulla oblongata, vagal ganglion, lateral line, otic vesicle cristae, otic vesicle maculae, fast muscle (weak)	This paper
y477Et	cfos:Gal4ff	n/a	statoacoustic ganglion, optic tectum - neuropil, medulla oblongata, fast muscle (weak), retina	This paper
y511Et	cfos:Gal4ff	1:12537737(-)z10 23115 bp from BX323837.1	preoptic area, hypothalamus - rostral zone, radial glia throughout brain, medulla oblongata, fast muscle (moderate), pLLg, pectoral fins	This paper
y512Et	SCP1:Gal4	n/a	optic tract - af9, hypothalamus - rostral zone, locus coeruleus, vagus motor neurons, facial octavolateralis motor neurons, aLLg, pLLg, lateral line, statoacoustic ganglion, heart (weak), muscle, notochord (weak), pectoral fin	This paper
y514Et	REx2-cfos:kGal4ff	n/a	subpallium, hypothalamus - rostral zone, facial sensory ganglion, torus semicircularis, habenula (left), vagal ganglion (and plexus in medulla oblongata), spinal cord	This paper
y515Et	REx2-cfos:kGal4ff	n/a	tegmentum, medulla oblongata (cluster of eng1b cells in ~rhombomere 7)	This paper
y532Et	cfos:Gal4ff	14:35798220(-)z10 Intron: BX511223.1	posterior tuberculum, ventral thalamus, optic tectum (cellular layer), tegmentum, dorsal raphe, horizontal myoseptum, integument (on eye), ocular muscle, fin	This paper
y533Et	SCP1:Gal4ff	1:46264212(-)z10 Intron: TMPRSS3	habenula (right, plus fasciculus retroflexus), floorplate, tegmentum, torus semicircularis, locus coeruleus, facial octavolateralis motor neurons (strong projections outside brain), fast muscle (moderate), projections to neuromasts (hair cell junctions)	This paper
y564Et	SCP1:Gal4ff	7:13657319(+)z10 Intron: slc39a1	posterior tuberculum, trigeminal ganglion, notochord, muscle, retina, spinal cord	This paper
y565Et	REx2-SCP1:Gal4ff	9:24606232(-)z10 4093 bp from tmeff2a	subpallium, medial habenula, thalamus, tegmentum, corpus cerebelli, cranial sensory ganglia, vagus motor neurons, inferior olive, aLLg (strong), pLLg, lateral line (branches to neuromasts), dorsal root ganglia (DRG), notochord (weak), muscle (weak)	This paper
y566Et	REx2-cfos:Gal4ff	9:34974048(+)z10 52835 bp from crlf2	thalamus, optic tectum (cellular layer), torus semicircularis, midbrain region dorsal to raphe, medulla oblongata (caudal region), jaw (basihyal) cartilage, esophagus,vagal ganglion,branchial arches,	This paper

y567Et	REx2-cfos:Gal4ff	n/a	retinal ganglion cells, retinotectal tract (strong), aLLg, pLLg, lateral line (plus innervation of neuromasts), spinal cord, lens (strong)	This paper
y575Et	cfos:Gal4	17:32648393(+)z10 Intron: eva1a	pretectum, pineal, hypothalamus - rostral zone, medulla oblongata, lateral line, pLLg, retina, spinal cord, notochord (weak), integument (weak)	This paper
y576Et	cfos:Gal4	8:14949268(-)z10 233 bp from fnbp1l	pineal, optic tectum, corpus cerebelli, tegmentum, medulla oblongata (lateral domain), endocrine pancreas (weak), retina (strong), fast muscle (weak)	This paper

Table S2. Summary of ZBB2 Gal4 enhancer trap lines
Coordinate system for mapped lines is either zv9 or zv10 as indicated.

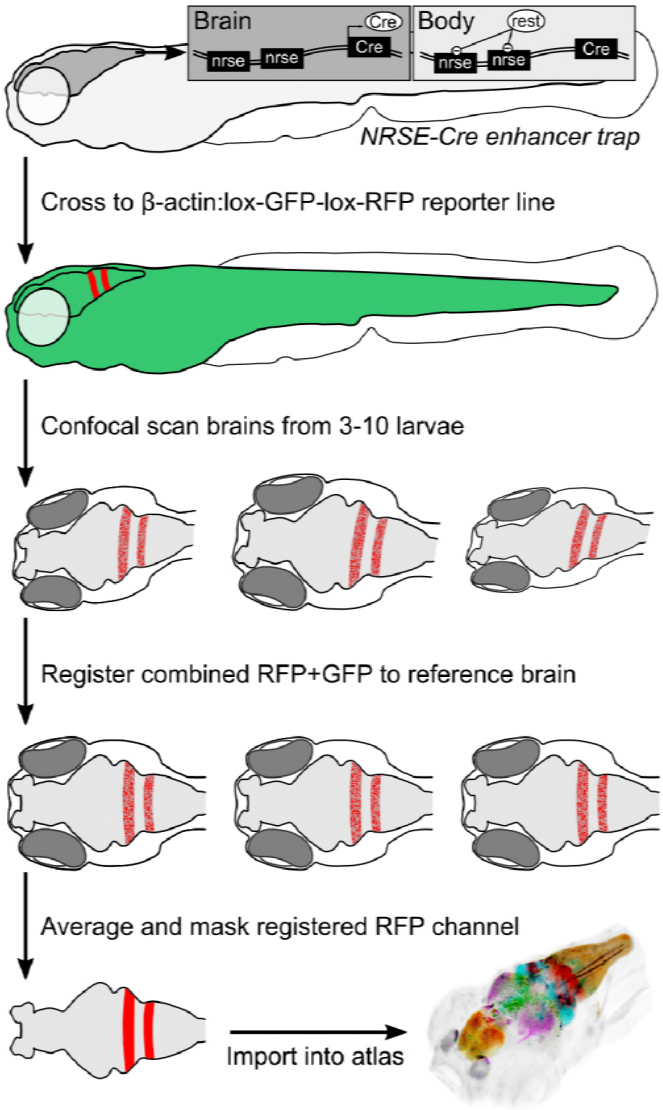

Figure 1. Procedure for imaging and co-registering new Cre lines

Inset schematics: neuronal-restrictive silencing element (nrse) sites in the enhancer trap construct are targets for the REST protein, which suppresses Cre expression outside the brain.

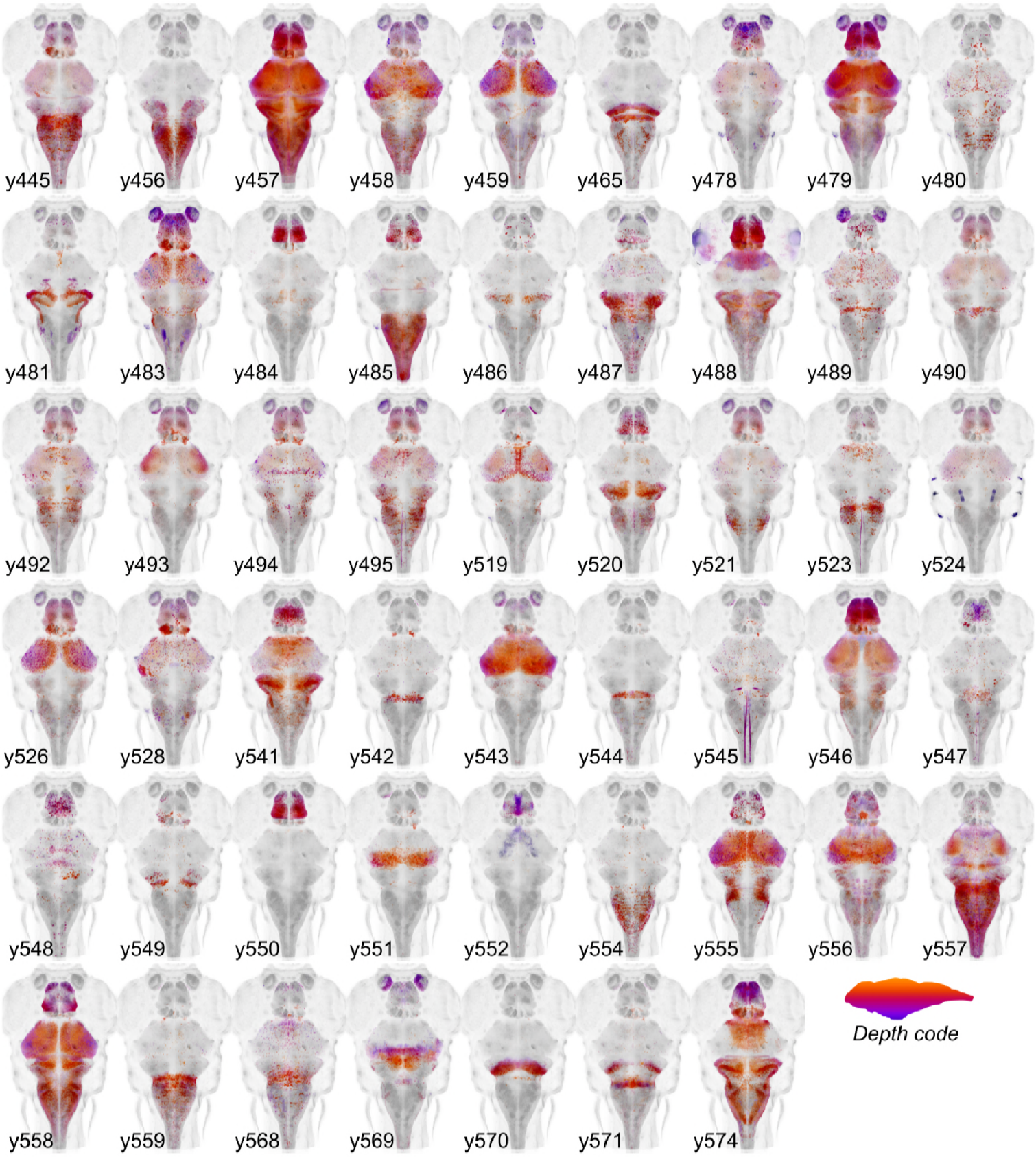

Figure 2. New Cre enhancer trap lines

Horizontal maximum projection of 52 new Cre enhancer trap lines, with color indicating depth along the dorsal-ventral dimension (huC counter-label, gray).

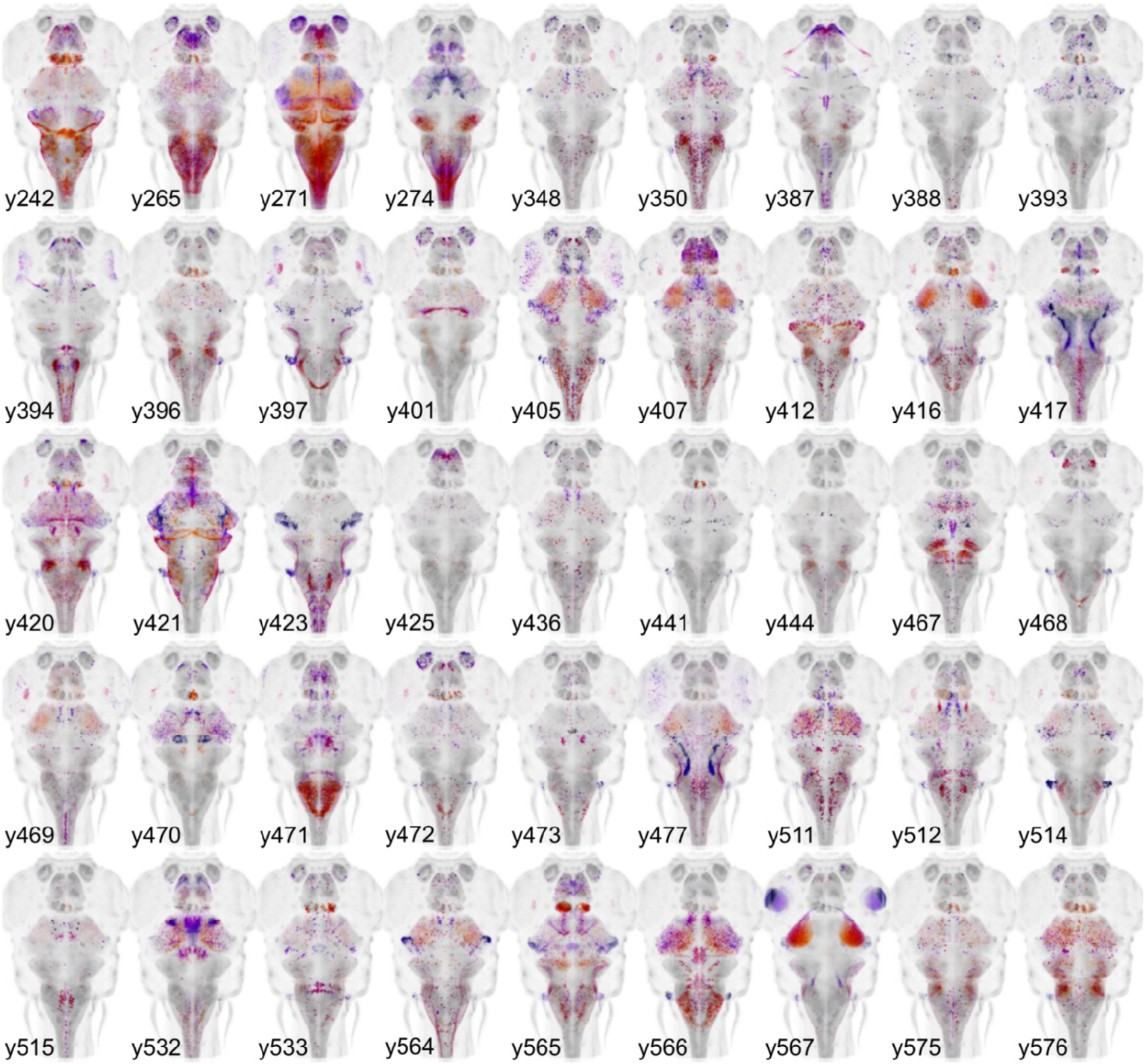

Figure 3. New Gal4 enhancer trap lines

Horizontal maximum projection of 45 new Gal4 enhancer trap lines (depth coded ; huC counter-label, gray)

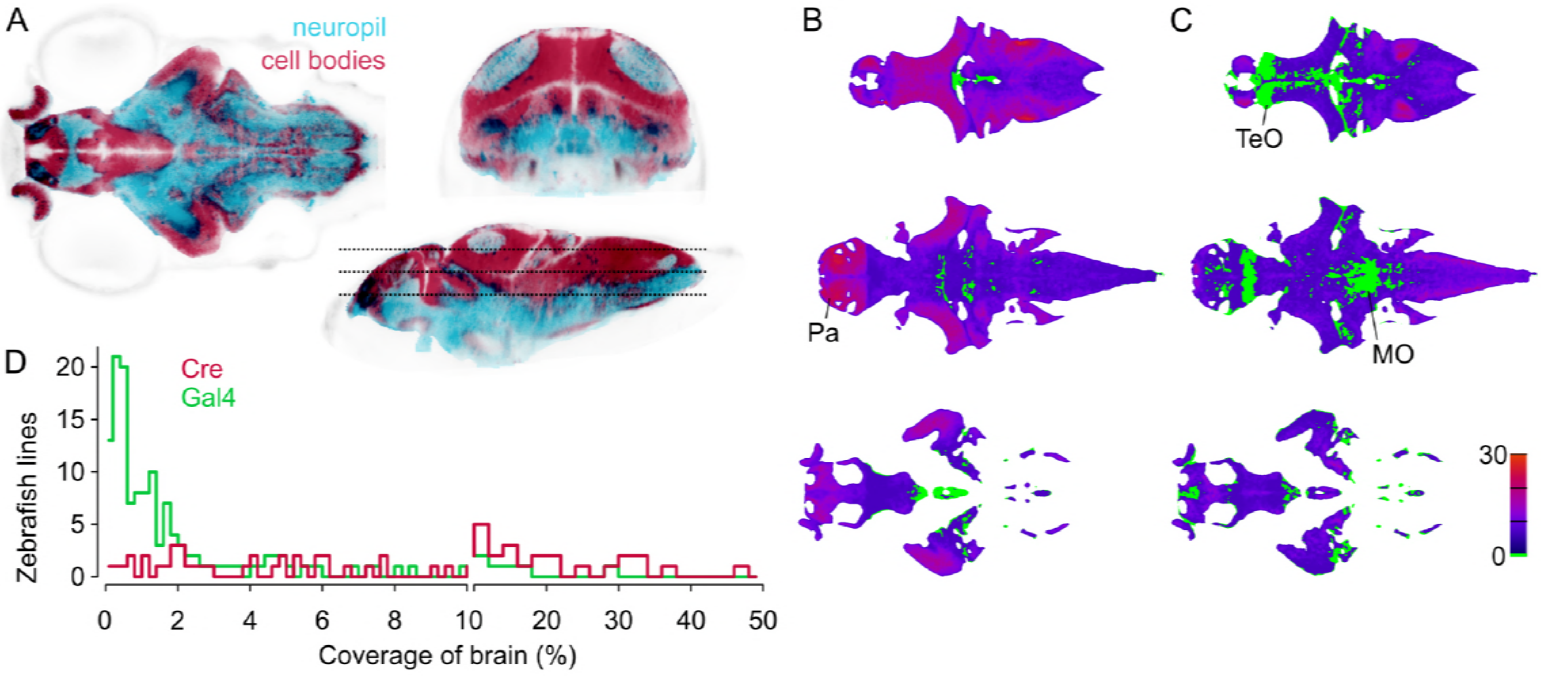

Figure 4. Spatial coverage of Cre and Gal4 enhancer trap lines

A. Horizontal (left), coronal (top right), sagittal (bottom right) sections showing *huC:nls-mCar* (cell bodies, red) and *huC:Gal4,UAS:syp-RFP* (neuropil, cyan) from ZBB (huC counter-label, gray), illustrating the separation of cell bodies and neuropil in 6 dpf brains.

B-C. Horizontal sections (at the levels indicated in A) of heat-maps showing the number of *et-Cre* (B) and *et-Gal4* (C) lines that label each voxel within the cellular area of the brain (scale bar, right). Voxels that lack coverage indicated in green. Coverage for Cre lines is highest in the pallium (Pa). Gal4 lines conspicuously lack coverage in the anterior optic tectum (TeO) and in a medial zone of the medulla oblongata (MO).

D. Histogram of the cellular-region coverage for *et-Cre* (red) and *et-Gal4* (green) lines.

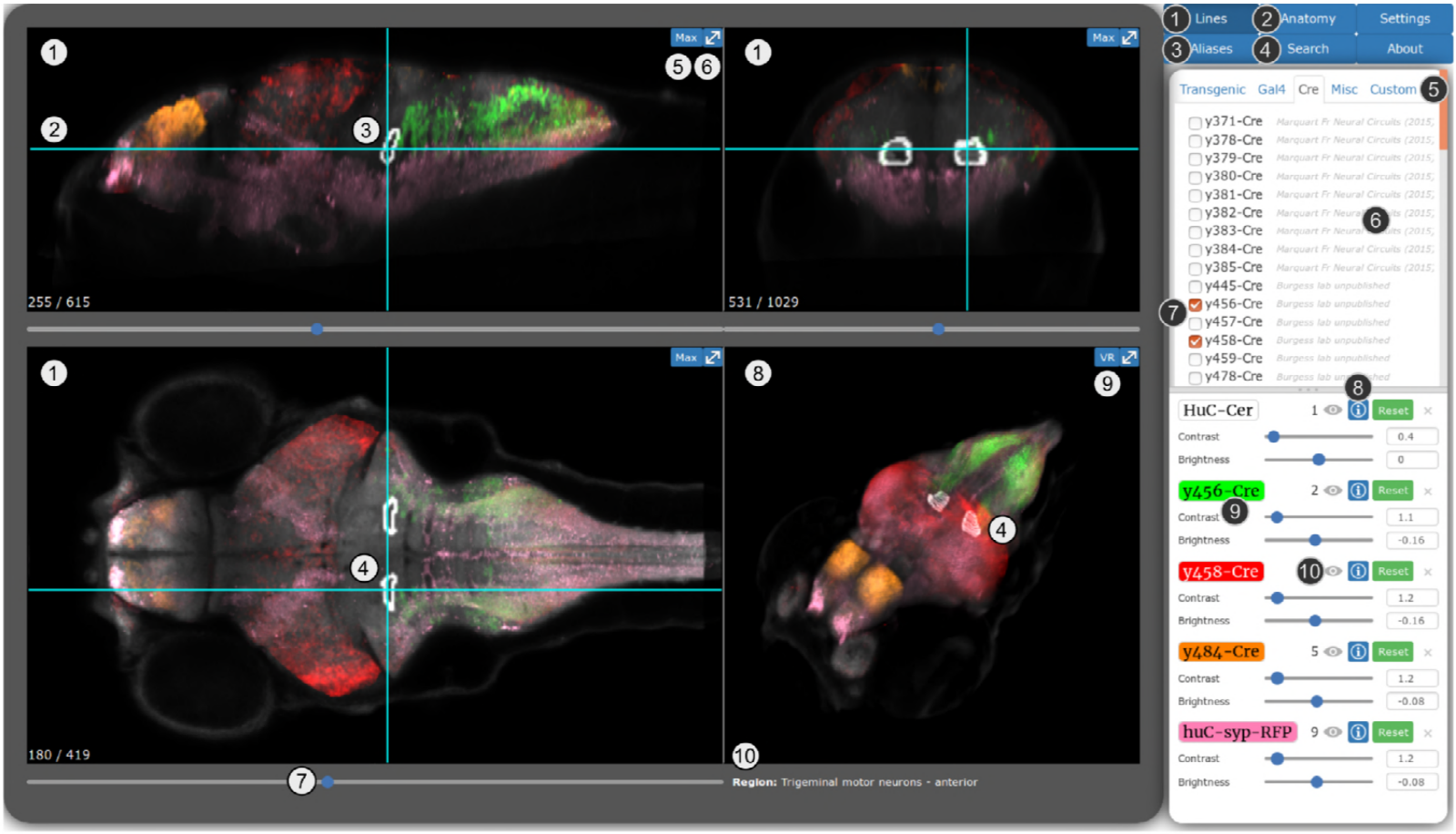

1. Panels for sagittal, coronal and horizontal views
2. Crosshairs indicate planes of section for other panels
3. Left-click updates slices shown in other two panels
4. Shift-click: anatomical region around selected voxel
5. Toggle single slice and projection views
6. Toggle panel and full window views
7. Sliders adjust plane of section
8. 3-D projection can be rotated using the mouse
9. Open virtual reality view of scene for cardboard viewer
10. Neuranatomical identity of selected voxel

1. Panel to select transgenic/Gal4/Cre lines
2. Panel to select anatomical regions
3. Panel to select lines that label key neurons/regions
4. Panel for spatial and text search functions
5. Load user-generated data
6. Link to publication describing selected line
7. Toggle display of selected line
8. Open window with links to ZFIN and Pubmed records
9. Adjust display color and intensity
10. Show/hide selected line, with keyboard shortcut

Figure 5. Web-browser interface for the Zebrafish Brain Browser
Online version of ZBB2, with key functions annotated. Panel size can be adjusted to best fit screen dimensions using the Settings menu.